3
Particle Phenomenology

In this chapter we shall look at some of the basic phenomena of particle physics – the properties of leptons and quarks, and the bound states of the latter, the hadrons. In later chapters we will discuss theories and models that attempt to explain these and other particle data.

3.1 Leptons

We have seen that the spin-$\frac{1}{2}$ leptons are one of the three classes of elementary particles in the standard model and we shall start with a discussion of their basic properties. Then we shall look in more detail at the neutral leptons, the neutrinos and, amongst other things, examine an interesting property they can exhibit, based on simple quantum mechanics, if they have non-zero masses.

3.1.1 Leptons multiplets and lepton numbers

There are six known leptons and they occur in pairs, called *generations*, which we write, for reasons that will become clear presently, as:

$$\begin{pmatrix} \nu_e \\ e^- \end{pmatrix}, \qquad \begin{pmatrix} \nu_\mu \\ \mu^- \end{pmatrix}, \qquad \begin{pmatrix} \nu_\tau \\ \tau^- \end{pmatrix}. \tag{3.1}$$

Each generation comprises a *charged lepton* with electric charge $-e$, and a *neutral neutrino*. The three charged leptons $(e^-,\ \mu^-,\ \tau^-)$ are the familiar electron, together with two heavier particles, the *mu lepton* (usually called the *muon,* or just *mu*) and the *tau lepton* (usually called the *tauon*, or just *tau*). The associated neutrinos are called the *electron neutrino*, *mu neutrino*, and *tau*

Nuclear and Particle Physics B. R. Martin
© 2006 John Wiley & Sons, Ltd. ISBN: 0-470-01999-9

neutrino, respectively.[1] In addition to the leptons, there are six corresponding antileptons:

$$\begin{pmatrix} e^+ \\ \bar{\nu}_e \end{pmatrix}, \quad \begin{pmatrix} \mu^+ \\ \bar{\nu}_\mu \end{pmatrix}, \quad \begin{pmatrix} \tau^+ \\ \bar{\nu}_\tau \end{pmatrix}. \tag{3.2}$$

Ignoring gravity, the charged leptons interact only via electromagnetic and weak forces, whereas for the neutrinos, only weak interactions have been observed.[2] Because of this, neutrinos, which are all believed to have extremely small masses, can be detected only with considerable difficulty.

The masses and lifetimes of the leptons are listed in Table 3.1. The electron and the neutrinos are stable, for reasons that will become clear shortly. The muons decay by the weak interaction processes

$$\mu^+ \to e^+ + \nu_e + \bar{\nu}_\mu \quad \text{and} \quad \mu^- \to e^- + \bar{\nu}_e + \nu_\mu, \tag{3.3a}$$

Table 3.1 Properties of leptons: all have spin $\frac{1}{2}$ and masses are given units of MeV/c^2; the antiparticles (not shown) have the same masses as their associated particles, but the electric charges (Q) and lepton numbers (L_ℓ , $\ell = e$, μ , τ) are reversed in sign

Name and symbol	Mass	Q	L_e	L_μ	L_τ	Lifetime (s)	Major decays
Electron e^-	0.511	-1	1	0	0	Stable	None
Electron neutrino ν_e	<2.2 eV/c^2	0	1	0	0	Stable	None
Muon (mu) μ^-	105.7	-1	0	1	0	2.197×10^{-6}	$e^-\bar{\nu}_e\nu_\mu$ (100%)
Muon neutrino ν_μ	<0.19	0	0	1	0	Stable	None
Tauon (tau) τ^-	1777.0	-1	0	0	1	2.906×10^{-13}	$\mu^-\bar{\nu}_\mu\nu_\tau$ (17.4%) $e^-\bar{\nu}_e\nu_\tau$ (17.8%) ν_τ+hadrons (~64%)
Tauon neutrino ν_τ	<18.2	0	0	0	1	Stable	None

with lifetimes $(2.19703 \pm 0.00004) \times 10^{-6}$ s. The tau also decays by the weak interaction, but with a much shorter lifetime $(2.906 \pm 0.011) \times 10^{-13}$ s. (This illustrates what we have already seen in nuclear physics, that lifetimes depend sensitively on the energy released in the decay, i.e. the Q-value.) Because it is heavier than the muon, the tau has sufficient energy to decay to many different final states, which can include both hadrons and leptons. However, about 35 per cent

[1] Leon Lederman, Melvin Schwartz and Jack Steinberger shared the 1988 Nobel Prize in Physics for their use of neutrino beams and the discovery of the muon neutrino. Martin Perl shared the 1995 Nobel Prize in Physics for his pioneering work in lepton physics and in particular for the discovery of the tau lepton.

[2] Although neutrinos have zero electric charge they could, in principle, have a charge *distribution* that would give rise to a magnetic moment (like neutrons) and hence electromagnetic interactions. This would of course be forbidden in the standard model because the neutrinos are defined to be point-like.

of decays again lead to purely leptonic final states, via reactions which are very similar to muon decay, for example:

$$\tau^+ \to \mu^+ + \nu_\mu + \bar{\nu}_\tau \quad \text{and} \quad \tau^- \to e^- + \bar{\nu}_e + \nu_\tau. \tag{3.3b}$$

Associated with each generation of leptons is a quantum number called a *lepton number*. The first of these lepton numbers is the *electron number*, defined for any state by

$$L_e \equiv N(e^-) - N(e^+) + N(\nu_e) - N(\bar{\nu}_e), \tag{3.4}$$

where $N(e^-)$ is the number of electrons present, $N(e^+)$ is the number of positrons present and so on. For single-particle states, $L_e = 1$ for e^- and ν_e, $L_e = -1$ for e^+ and $\bar{\nu}_e$, and $L_e = 0$ for all other particles. The *muon* and *tauon numbers* are defined in a similar way and their values for all single particle states are summarized in Table 3.1. They are zero for all particles other than leptons. For multiparticle states, the lepton numbers of the individual particles are simply added. For example, the final state in neutron β-decay (i.e. $n \to p + e^- + \bar{\nu}_e$) has

$$L_e = L_e(p) + L_e(e^-) + L_e(\bar{\nu}_e) = (0) + (1) + (-1) = 0, \tag{3.5}$$

like the initial state, which has $L_e(n) = 0$.

In the standard model, the value of each lepton number is postulated to be conserved in *any* reaction. The decays (3.3) illustrate this principle of *lepton number conservation*. Until recently this was considered an absolute conservation law, but in Section 3.1.4 we will discuss growing evidence that neutrinos are not strictly massless, which would imply that conservation of individual lepton numbers is not an exact law. However, for the present we will assume lepton numbers are conserved, as in the standard model. In electromagnetic interactions, this reduces to the conservation of $N(e^-) - N(e^+)$, $N(\mu^-) - N(\mu^+)$ and $N(\tau^-) - N(\tau^+)$, since neutrinos are not involved. This implies that the charged leptons can only be created or annihilated in particle–antiparticle pairs. For example, in the electromagnetic reaction

$$e^+ + e^- \to \mu^+ + \mu^- \tag{3.6}$$

an electron pair is annihilated and a muon pair is created by the mechanism of Figure 3.1.

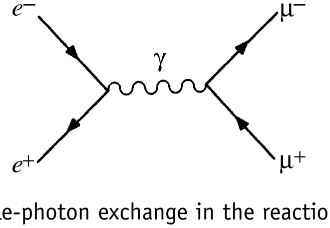

Figure 3.1 Single-photon exchange in the reaction $e^+e^- \to \mu^+\mu^-$

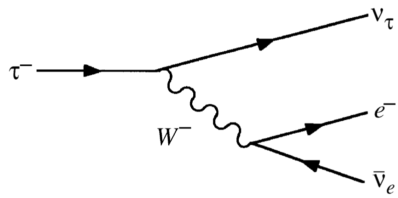

Figure 3.2 Dominant Feynman diagram for the decay $\tau^- \to e^-\bar{\nu}_e\nu_\tau$

In weak interactions more general possibilities are allowed, which still conserve lepton numbers. For example, in the tau-decay process $\tau^- \to e^- + \bar{\nu}_e + \nu_\tau$, a tau converts to a tau neutrino and an electron is created together with an antineutrino, rather than a positron. The dominant Feynman graph corresponding to this process is shown in Figure 3.2.

Lepton number conservation, like electric charge conservation, plays an important role in understanding reactions involving leptons. Observed reactions conserve lepton numbers, while reactions that do not conserve lepton numbers are 'forbidden' and are not observed. For example, the neutrino scattering reaction

$$\nu_\mu + n \to \mu^- + p \tag{3.7}$$

is observed experimentally, while the apparently similar reaction

$$\nu_\mu + n \to e^- + p, \tag{3.8}$$

which violates both L_e and L_μ conservation, is not. Another example which violates both L_e and L_μ conservation is $\mu^- \to e^- + \gamma$. If this reaction were allowed, the dominant decay of the muon would be electromagnetic and the muon lifetime would be much shorter than its observed value. This is very strong evidence that even if lepton numbers are not absolutely conserved, they are conserved to a high degree of accuracy.

Finally, conservation laws explain the stability of the electron and the neutrinos. The electron is stable because electric charge is conserved in all interactions and the electron is the lightest charged particle. Hence decays to lighter particles that satisfy all other conservation laws, like $e^- \to \nu_e + \gamma$, are necessarily forbidden by electric charge conservation. In the same way, lepton number conservation implies that the lightest particles with non-zero values of the three lepton numbers – the three neutrinos – are stable, whether they have zero masses or not. Of course, if lepton numbers are not conserved, then the latter argument is invalid.

3.1.2 Neutrinos

As we mentioned in Chapter 1, the existence of the *electron neutrino* ν_e was first postulated by Pauli in 1930. He did this in order to understand the observed nuclear β-decays

$$(Z\,,\,N) \rightarrow (Z+1,\,N-1) + e^- + \bar{\nu}_e \tag{3.9}$$

and

$$(Z,\,N) \rightarrow (Z-1,\,N+1) + e^+ + \nu_e \tag{3.10}$$

that were discussed in Chapter 2. The neutrinos and antineutrinos emitted in these decays are not observed experimentally, but are inferred from energy and angular momentum conservation. In the case of energy, if the antineutrino were not present in the first of the reactions, the energy E_e of the emitted electron would be a unique value equal to the difference in rest energies of the two nuclei, i.e.

$$E_e = \Delta Mc^2 = [M(Z,\,N) - M(Z+1,\,N-1)]c^2, \tag{3.11}$$

where for simplicity we have neglected the extremely small kinetic energy of the recoiling nucleus. However, if the antineutrino is present, the electron energy would not be unique, but would lie in the range

$$m_e c^2 \leq E_e \leq (\Delta M - m_{\bar{\nu}_e})c^2, \tag{3.12}$$

depending on how much of the kinetic energy released in the decay is carried away by the neutrino. Experimentally, the observed energies span the whole of the above range and in principle a measurement of the energy of the electron near its maximum value of $E_e = (\Delta M - m_{\bar{\nu}_e})c^2$ determines the neutrino mass. The most accurate results come from tritium decay and are compatible with zero mass for electron antineutrinos. When experimental errors are taken into account, the experimentally allowed range is

$$0 \leq m_{\bar{\nu}_e} < 2.2\,\mathrm{eV/c^2} \approx 4.3 \times 10^{-6} m_e. \tag{3.13}$$

We will discuss this experiment in more detail in Chapter 7, after we have considered the theory of β-decay.

The masses of both ν_μ and ν_τ can similarly be directly inferred from the e^- and μ^- energy spectra in the leptonic decays of muons and tauons, using energy conservation. The results from these and other decays show that the neutrino masses are very small compared with the masses of the associated charged leptons. The present limits are given in Table 3.1.

Small neutrino masses, compatible with the above limits, can be ignored in most circumstances, and there are theoretical attractions in assuming neutrino masses are precisely zero, as is done in the standard model. However, we will show in the following section that there is now strong evidence for physical phenomena that could not occur if the neutrinos had exactly zero mass. The consequences of neutrinos having small masses have therefore to be taken seriously.

Because neutrinos only have weak interactions, they can only be detected with extreme difficulty. For example, electron neutrinos and antineutrinos of sufficient energy can in principle be detected by observing the *inverse β-decay* processes

$$\nu_e + n \to e^- + p \tag{3.14}$$

and

$$\bar{\nu}_e + p \to e^+ + n\,. \tag{3.15}$$

However, the probability for these and other processes to occur is extremely small. In particular, the neutrinos and antineutrinos emitted in β-decays, with energies of the order of 1 MeV, have mean free paths in matter of the order of 10^6 km.[3] Nevertheless, if the neutrino flux is intense enough and the detector is large enough, the reactions can be observed. In particular, uranium fission fragments are neutron rich, and decay by electron emission to give an antineutrino flux that can be of the order of $10^{17}\,\mathrm{m}^{-2}\,\mathrm{s}^{-1}$ or more in the vicinity of a nuclear reactor, which derives its energy from the decay of nuclei. These antineutrinos will occasionally interact with protons in a large detector, enabling examples of the inverse β-decay reaction to be observed. As mentioned in Chapter 1 (Footnote 12), electron neutrinos were first detected in this way by Reines and Cowan in 1956, and their interactions have been studied in considerable detail since.

The mu neutrino, ν_μ, has been detected using the reaction $\nu_\mu + n \to \mu^- + p$ and other reactions. In this case, well-defined high-energy ν_μ beams can be created in the laboratory by exploiting the decay properties of *pions*, which are particles we have mentioned briefly in Chapter 1 and which we will meet in more detail presently. The probability of neutrinos interacting with matter increases rapidly with energy (this will be demonstrated in Section 6.5.2) and, for large detectors, events initiated by such beams are so copious that they have become an indispensable tool in studying both the fundamental properties of weak interactions and the internal structure of the proton. Finally, in 2000, a few examples of tau neutrinos were reported, so that almost 70 years after Pauli first suggested the existence of a neutrino, all three types had been directly detected.

3.1.3 Neutrino mixing and oscillations

Neutrinos are assumed to have zero mass in the standard model. However, as mentioned above, data from the β-decay of tritium are compatible with a non-zero

[3]The mean free path is the distance a particle would have to travel in a medium for there to be a significant probability of an interaction. A formal definition is given in Chapter 4.

mass. A phenomenon that can occur if neutrinos have non-zero masses is *neutrino mixing*. This arises if we assume that the observed neutrino states ν_e, ν_μ and ν_τ which take part in weak interactions, i.e. the states that couple to electrons, muons and tauons, respectively, are not eigenstates of mass, but instead are linear combinations of three other states ν_1, ν_2 and ν_3 which do have definite masses m_1, m_2 and m_3, i.e. *are* eigenstates of mass. For algebraic simplicity we will consider the case of mixing between just two states, one of which we will assume is ν_μ and the other we will denote by ν_x. Then, in order to preserve the orthonormality of the states, we can write

$$\nu_\mu = \nu_1 \cos\alpha + \nu_2 \sin\alpha \tag{3.16}$$

and

$$\nu_x = -\nu_1 \sin\alpha + \nu_2 \cos\alpha. \tag{3.17}$$

Here α is a *mixing angle* which must be determined from experiment. If $\alpha \neq 0$ then some interesting predictions follow.

Measurement of the mixing angle may be made in principle by studying the phenomenon of *neutrino oscillation*. When, for example, a muon neutrino is produced with momentum $\mathbf{p}$ at time $t = 0$, the ν_1 and ν_2 components will have slightly different energies E_1 and E_2 due to their slightly different masses. In quantum mechanics, their associated waves will therefore have slightly different frequencies, giving rise to a phenomenon somewhat akin to the 'beats' heard when two sound waves of slightly different frequency are superimposed. As a result of this, one finds that the original beam of muon neutrinos develops a ν_x component whose intensity oscillates as it travels through space, while the intensity of the muon neutrino beam itself is correspondingly reduced, i.e. muon neutrinos will 'disappear'.

This effect follows from simple quantum mechanics. To illustrate this we will consider a muon neutrino produced with momentum $\mathbf{p}$ at time $t = 0$. The initial state is therefore

$$\left|\nu_\mu, \mathbf{p}\right\rangle = |\nu_1, \mathbf{p}\rangle \cos\alpha + |\nu_2, \mathbf{p}\rangle \sin\alpha, \tag{3.18}$$

where we use the notation $|P, \mathbf{p}\rangle$ to denote a state of a particle P having momentum $\mathbf{p}$. After time t this will become

$$a_1(t)\,|\nu_1, \mathbf{p}\rangle \cos\alpha + a_2(t)|\nu_2, \mathbf{p}\rangle \sin\alpha, \tag{3.19}$$

where

$$a_i(t) = \mathrm{e}^{-iE_i t/\hbar} \qquad (i = 1, 2) \tag{3.20}$$

are the usual oscillating energy factors associated with any quantum mechanical stationary state.[4] For $t \neq 0$, the linear combination (3.19) does not correspond to a pure muon neutrino state, but can be written as a linear combination

$$A(t)\big|\nu_\mu,\, \mathbf{p}\big\rangle + B(t)|\nu_x,\, \mathbf{p}\rangle, \tag{3.21}$$

of ν_μ and ν_x states, where the latter is

$$|\nu_x,\, \mathbf{p}\rangle = -|\nu_1,\, \mathbf{p}\rangle \sin\alpha + |\nu_2,\, \mathbf{p}\rangle \cos\alpha. \tag{3.22}$$

The functions $A(t)$ and $B(t)$ are found by solving Equations (3.18) and (3.22) for $|\nu_1,\, \mathbf{p}\rangle$ and $|\nu_2,\, \mathbf{p}\rangle$, then substituting the results into (3.19) and comparing at with (3.21). This gives,

$$A(t) = a_1(t)\cos^2\alpha + a_2(t)\sin^2\alpha \tag{3.23}$$

and

$$B(t) = \sin\alpha\cos\alpha\,[a_2(t) - a_1(t)]. \tag{3.24}$$

The probability of finding a ν_x state is therefore

$$P(\nu_\mu \to \nu_x) = |B(t)|^2 = \sin^2(2\alpha)\sin^2[(E_2 - E_1)\,t/2\hbar] \tag{3.25}$$

and thus oscillates with time, while the probability of finding a muon neutrino is reduced by a corresponding oscillating factor. Similar effects are predicted if instead we start from electron or tau neutrinos. In each case the oscillations vanish if the mixing angle is zero, or if the neutrinos have equal masses, and hence equal energies, as can be seen explicitly from Equation (3.25). In particular, such oscillations are not possible if the neutrinos both have zero masses.

Returning to Equation (3.25), since neutrino masses are very small, $E_{1,2} \gg m_i c^2$ $(i = 1,\, 2)$ and we can write

$$E_2 - E_1 = \left(m_2^2c^4 + p^2c^2\right)^{1/2} - \left(m_1^2c^4 + p^2c^2\right)^{1/2} \approx \frac{m_2^2c^4 - m_1^2c^4}{2pc}. \tag{3.26}$$

Also, $E \approx pc$ and $t \approx |\mathbf{x}|/c \equiv L/c$, where L is the distance from the point of production. Thus Equation (3.25) may be written

$$P(\nu_\mu \to \nu_x) \approx \sin^2(2\alpha)\sin^2\left[\frac{\Delta(m^2c^4)L}{4\hbar cE}\right], \tag{3.27a}$$

[4] See, for example, Chapter 1 of Ma92.

with

$$P(\nu_\mu \to \nu_\mu) = 1 - P(\nu_\mu \to \nu_x), \tag{3.27b}$$

where $\Delta(m^2c^4) \equiv m_2^2c^4 - m_1^2c^4$. These formulae assume that the neutrinos are propagating in a vacuum, whereas in real experiments they will be passing through matter and the situation is more complicated than these simple results suggest. This formalism can be extended to the general case of mixing between all three neutrino species, but at the expense of additional free parameters.[5]

Attempts to establish neutrino oscillations rest on using the inverse β-decay reactions (3.14) and (3.15) to produce electrons and the analogous reactions for muon neutrinos to produce muons, which are then detected. In addition, the time t is determined by the distance of the neutrino detector from the source of the neutrinos, since their energies are always much greater than their possible masses, and they travel at approximately the speed of light. Hence, for example, if we start with a source of muon neutrinos, the flux of muons observed in a detector should vary with its distance from the source of the neutrinos, if appreciable oscillations occur. In practice, oscillations at the few per cent level are very difficult to detect for experimental reasons that we will not discuss here.

3.1.4 Neutrino masses

There are a number of different types of experiment that can explore neutrino oscillations and hence neutrino masses. The first of these to produce definitive evidence for oscillations was that of a Japanese group in 1998 using the giant *Super Kamiokande* detector to study *atmospheric neutrinos* produced by the action of cosmic rays.[6] (Neutrinos of each generation are often referred to as having a different *flavour* and so the observations are evidence for flavour oscillation.)

The *Super Kamiokande* detector is shown in Figure 3.3. (Detectors will be discussed in detail in Chapter 4, so the description here will be brief.) It consists of a stainless steel cylindrical tank of roughly 40 m diameter and 40 m height, containing about 50 000 metric tons of very pure water. The detector is situated deep underground in a mountain in Japan, at a depth equivalent to 2700 m of water. This is to use the rocks above to shield the detector from cosmic ray muons. The volume is separated into a large inner region, the walls of which are lined with 11 200 light-sensitive devices called photomultipliers (the physics of these will be discussed in Chapter 4). These register the presence of electrons or muons

[5]See, for example, the Review of Particle Properties published biannually by the Particle Data Group (2004 edition: Ei04). The PDG Review is also available at http://pdg.lbl.gov. This publication contains a wealth of useful data about elementary particles and their interactions and we will refer to it in future simply as PDG04.

[6]Cosmic neutrinos were first detected (independently) by Raymond Davis Jr. and Masatoshi Koshiba, for which they were jointly awarded the 2002 Nobel Prize in Physics.

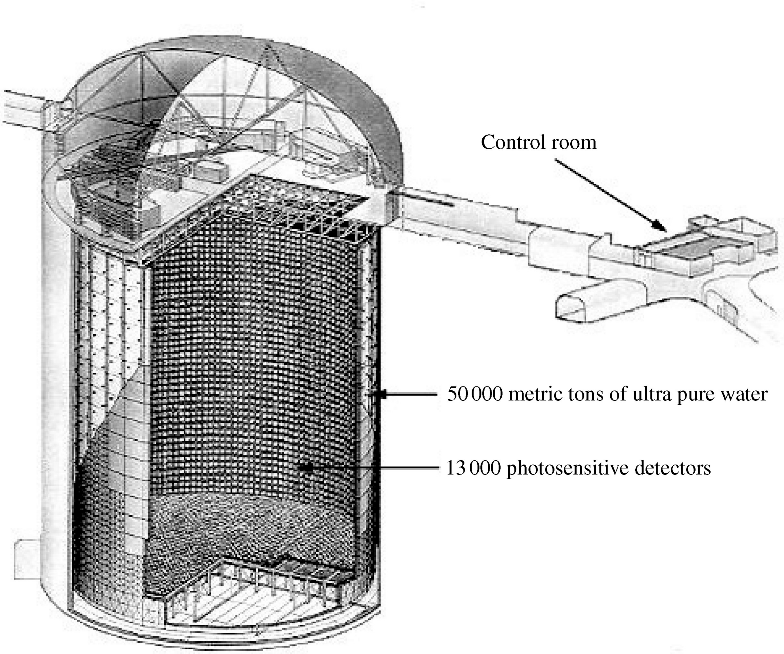

Figure 3.3 A schematic diagram of the *Super Kamiokande* detector (adapted from an original University of Hawaii, Manoa, illustration -- with permission)

indirectly by detecting the light (the so-called Čerenkov radiation – again, see Chapter 4) emitted by relativistic charged particles (the electrons or muons) that are created in, or pass through, the water. The outer region of water acts as a shield against low-energy particles entering the detector from outside. An additional 1200 photomultipliers are located there to detect muons that enter or exit the detector.

When cosmic ray protons collide with atoms in the upper atmosphere they create many pions, which in turn create neutrinos mainly by the decay sequences

$$\pi^- \to \mu^- + \bar{\nu}_\mu, \quad \pi^+ \to \mu^+ + \nu_\mu \tag{3.28}$$

and

$$\mu^- \to e^- + \bar{\nu}_e + \nu_\mu, \quad \mu^+ \to e^+ + \nu_e + \bar{\nu}_\mu. \tag{3.29}$$

From this, one would naively expect to detect two muon neutrinos for every electron neutrino. However, the ratio was observed to be about 1.3 to 1 on average, suggesting that the muon neutrinos produced might be oscillating into other species.

Clear confirmation for this was found by exploiting the fact that the detector could measure the direction of the detected neutrinos to study the azimuthal dependence of the effect. Since the flux of cosmic rays that lead to neutrinos with energies above about 1 GeV is isotropic, the production rate for neutrinos should be the same all around the Earth. In particular, one can compare the measured flux from neutrinos produced in the atmosphere directly above the detector, which have a short flight path before detection, with those incident from directly below, which have travelled a long way through the Earth before detection, and so have had plenty of time to oscillate (perhaps several cycles). Experimentally, it was found that the yield of electron neutrinos from above and below were the same within errors and consistent with the expectation for no oscillations. However, while the yield of muon neutrinos from above accorded with the expectation for no significant oscillations, the flux of muon neutrinos from below was a factor of about two lower. This is clear evidence for muon neutrino oscillations.

In a later development of the experiment, the flux of muon neutrinos was measured as a function of L/E by estimating L from the reconstructed neutrino direction. Values of L range from 15 km to 13000 km. The results are shown in Figure 3.4 in the form of the ratio of observed number of events to the theoretical expectation if there were no oscillations. The data show clear evidence for a deviation of this ratio from unity, particularly at large values of L/E.

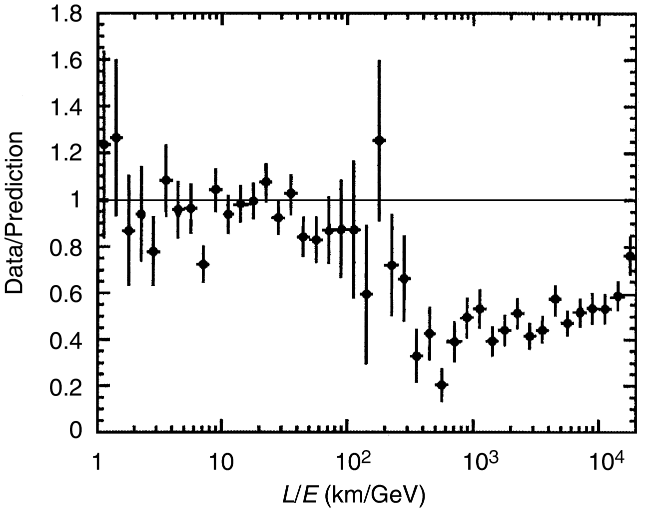

Figure 3.4 Data from the *Super Kamiokande* detector showing evidence for neutrino oscillations in atmospheric neutrinos (adapted from As04, copyright American Physical Society)

Other experiments also set limits on $P(\nu_\mu \to \nu_e)$ and taking these into account the most plausible hypothesis is that muon neutrinos are changing into tau neutrinos, which for the neutrino energies concerned could not be detected by Super Kamiokande. The data are consistent with this hypothesis and yield the values

$$1.9 \times 10^{-3} \leq \Delta(m^2c^4) \leq 3.0 \times 10^{-3}\ (\text{eV})^2, \quad \sin^2(2\alpha) > 0.9 \tag{3.30}$$

at 90 per cent confidence level. This conclusion is supported by preliminary results from laboratory-based experiments that start with a beam of ν_μ and measure the flux at a large distance (250 km) from the origin. Analysis of the data yields similar parameters to those above.

A second piece of evidence for neutrino oscillations comes from our knowledge of the Sun. We shall see in Chapter 8 that the energy of the Sun is due to various nuclear reactions and these produce a huge flux of electron neutrinos that can be detected at the surface of the Earth. Since the astrophysics of the Sun and nuclear production processes are well understood, this flux can be calculated with some confidence by what is known as the standard solar model.[7] However, the measured count rate is about a factor of two lower than the theoretical expectation. This is the so-called *solar neutrino problem*. It was first investigated by Davis and co-workers in the late 1960s who studied the reaction

$$\nu_e + {}^{37}\mathrm{Cl} \rightarrow {}^{37}\mathrm{Ar} + e^-, \tag{3.31}$$

to detect the neutrinos. (This required sensitive radiochemical analysis to confirm the production of ${}^{37}\mathrm{Ar}$.) This reaction has a threshold of 0.81 MeV and is therefore only sensitive to relatively high-energy neutrinos from the Sun. Such neutrinos come predominantly from the weak interaction decay

$$ {}^{8}\mathrm{B} \rightarrow {}^{8}\mathrm{Be} + e^+ + \nu_e, \tag{3.32}$$

where the neutrinos have an average energy $\sim 7\,\mathrm{MeV}$. More recent experiments have studied the same process using the reactions

$$\text{(a)}\ \nu_x + d \rightarrow e^- + p + p, \quad \text{(b)}\ \nu_x + d \rightarrow \nu_x + p + n, \quad \text{(c)}\ \nu_x + e^- \rightarrow \nu_x + e^-, \tag{3.33}$$

to detect the neutrinos, where d is a deuteron. The first of these reactions clearly can be initiated with electron neutrinos only, whereas the other two can be initiated with neutrinos of any flavour. The measured flux of ν_e from reaction (a) agrees well with the standard solar model, but the ratio of the flux for ν_e to that for ν_x, where x could be a combination of μ and τ, obtained by using data from all three reactions, is less than unity. For example, the Sudbury Neutrino Observatory (SNO) experiment finds a ratio of about 0.3. Thus there is a flux of neutrinos of a type that did not come from the original decay process. The observations are further clear evidence for flavour oscillation.

Although the neutrinos from (3.32) have been extensively studied, this decay contributes only about 10^{-4} of the total solar neutrino flux. It is therefore important

[7] See, for example, Chapter 4 of Ph94.

to detect neutrinos from other reactions and in particular from the reaction

$$p + p \to d + e^+ + \nu_e, \tag{3.34}$$

which is the primary reaction that produces the energy of the Sun and contributes approximately 90 per cent of the solar neutrino flux. (It will be discussed in more detail in Chapter 8.) The neutrinos in this reaction have average energies of $\sim$0.26 MeV and so cannot be detected by reaction (3.31). Instead, the reaction

$$\nu_e + {}^{71}\mathrm{Ga} \to {}^{71}\mathrm{Ge} + e^- \tag{3.35}$$

has been used, which has a threshold of 233 keV. (The experiments can also detect neutrinos from the solar reaction $e^- + {}^7\mathrm{Be} \to {}^7\mathrm{Li} + \nu_e$.) Just as for the original experiments of Davis *et al.*, there are formidable problems in identifying the radioactive products from this reaction, which produces only about 1 atom of ^{71}Ge per day in a target of 30 tons of gallium. Nevertheless, results from these experiments confirm the deficit of electron neutrinos and find between 60 and 70 per cent of the flux expected from the standard solar model without flavour changing.

These solar neutrino results require that interactions with matter play a significant role in flavour changing and imply, for example, that a substantial fraction of a beam of $\bar{\nu}_e$ would change to antineutrinos of other flavours after travelling a distance of the order of 100 km from its source. This prediction has been tested by the KamLAND group in Japan. They have studied the $\bar{\nu}_e$ flux from more than 60 reactors in Japan and South Korea after the neutrinos have travelled distances of between 150 and 200 km. They found that the $\bar{\nu}_e$ flux was only about 60 per cent of that expected from the known characteristics of the reactors. A simultaneous analysis of the data from this experiment and the solar neutrino data yields the result:

$$7.6 \times 10^{-5} \le \Delta(m^2c^4) \le 8.8 \times 10^{-5}\,(\mathrm{eV})^2, \quad 0.32 \le \tan^2(\alpha) \le 0.48. \tag{3.36}$$

The existence of neutrino oscillations (flavour changing), and by implication non-zero neutrino masses, is now generally accepted on the basis of the above set of experiments.

What are the consequences of these results for the standard model? The observation of oscillations does not lead to a measurement of the neutrino masses, only (squared) mass differences, but combined with the tritium β-decay experiment, it would be natural to assume that neutrinos all had very small masses, with the mass differences being of the same order-of-magnitude as the masses themselves. The standard model can be modified to accommodate small masses, although methods for doing this are not without their own problems.[8] Unfortunately, the various

[8]One possibility will be mentioned briefly in Chapter 9 as part of a discussion of the general question of how masses arise in the standard model.

experiments – although producing compatible values for the mixing angle $\alpha \sim 40^\circ$ – yield wildly different values for the mass difference, as can be seen from Equations (3.30) and (3.36). However, the analyses have been made in the framework of a two-component mixing model, whereas there are of course three neutrinos. Thus it could be, for example, that two of the neutrino states are separated by a small mass difference given by Equation (3.36) and the third is separated from them by a relatively large mass difference given by Equation (3.30). Progress will have to await experiments currently being planned to detect oscillations directly using prepared neutrino beams and which will make measurements at great distances from their origin. These experiments are expected to produce data in the next few years and should yield definitive values of the neutrino mass differences and the various mixing angles involved.[9]

The consequences for lepton number conservation are unclear. In the simple mixing model above, the total lepton number could still be conserved, but individual lepton numbers would not. However, there are other theoretical descriptions of neutrino oscillations and this is an open question. A definitive answer would be to detect *neutrinoless double β-decay*, such as

$$^{76}\mathrm{Ge} \to {}^{76}\mathrm{Se} + 2e^-, \tag{3.37}$$

where the final state contains two electrons, but no antineutrinos. This could occur if the neutrino emitted by the parent nucleus was internally absorbed by the daughter nucleus (i.e. it never appears as a real particle) which is possible only if $\nu_e \equiv \bar{\nu}_e$. A very recent experiment claims to have detected this decay, but the result is not universally accepted and at present 'the jury is out'. Experiments planned for the next few years should settle important questions about lepton number conservation and the nature of neutrinos.

3.1.5 Universal lepton interactions – the number of neutrinos

The three neutrinos have similar properties, but the three charged leptons are strikingly different. For example: the mass of the muon is roughly 200 times greater than that of the electron and consequently its magnetic moment is 200 times smaller; high-energy electrons are stopped by modest thicknesses of a centimetre or so of lead, while muons are the most penetrating form of radiation known, apart from neutrinos; and the tauon lifetime is many orders of magnitude smaller than the muon lifetime, while the electron is stable. It is therefore a remarkable fact that all experimental data are consistent with the assumption that the interactions of the electron and its associated neutrino are identical to those of the muon and its associated neutrino and of the tauon and its neutrino, *provided the*

[9]For a review of these experiments see, for example, http://www.hep.anl.gov/ndk/hypertext/nuindustry.html.

mass differences are taken into account. This property, called *lepton universality*, can be verified with great precision, because we have a precise theory of electromagnetic and weak interactions (to be discussed in Chapter 6), which enables predictions to be made of the mass dependence of all observables.

For example, when we discuss experimental methods in Chapter 4, we will show that the *radiation length*, which is a measure of how far a charged particle travels through matter before losing a certain fraction of its energy by radiation, is proportional to the squared mass of the radiating particle. Hence it is about 4×10^4 times greater for muons than for electrons, explaining their much greater penetrating power in matter. As another example, we have seen that the rates for weak β-decays are extremely sensitive to the kinetic energy released in the decay (recall the enormous variation in the lifetimes of nuclei decaying via β-decay). From dimensional arguments and the fact that they are weak interactions, the rates for muon and tau leptonic decays are predicted to be proportional to the fifth power of the relevant Q-values multiplied by G_F^2, the square of the Fermi coupling.[10] Thus, from universality, the ratio of the decay rates Γ is given approximately by

$$\frac{\Gamma(\tau^- \to e^- + \bar{\nu}_e + \nu_\tau)}{\Gamma(\mu^- \to e^- + \bar{\nu}_e + \nu_\mu)} \approx \left(\frac{Q_\tau}{Q_\mu}\right)^5 = 1.37 \times 10^6. \tag{3.38}$$

This is in excellent agreement with the experimental value of 1.35×10^6 (and is even closer in a full calculation) and accounts very well for the huge difference between the tau and muon lifetimes. The above are just some of the most striking manifestations of the universality of lepton interactions.

A question that arises naturally is whether there are more generations of leptons, with identical interactions, waiting to be discovered. This question has been answered, under reasonable assumptions, by an experimental study of the decays of the Z^0 boson. This particle, one of the two gauge bosons associated with the weak interaction, has a mass of 91 GeV/c^2. It decays, among other final states, to neutrino pairs

$$Z^0 \to \nu_\ell + \bar{\nu}_\ell \qquad (\ell = e,\ \mu,\ \tau). \tag{3.39}$$

If we assume universal lepton interactions and neutrino masses which are small compared with the mass of the Z^0,[11] the decay rates to a given neutrino pair will all be equal and thus

$$\Gamma_{\text{neutrinos}} \equiv \Gamma_{\nu_e} + \Gamma_{\nu_\mu} + \Gamma_{\nu_\tau} + \ \cdots \ = N_\nu \Gamma_\nu, \tag{3.40}$$

[10]The increase of the decay rate as the fifth power of Q is known as *Sargent's Rule*.
[11]More precisely, we assume $m_\nu \leq M_Z/2$, so that the decays $Z \to \nu\bar{\nu}$ are not forbidden by energy conservation.

where N_ν is the number of neutrino species and Γ_ν is the decay rate to any given pair of neutrinos. The measured total decay rate may then be written

$$\Gamma_{\text{total}} = \Gamma_{\text{hadrons}} + \Gamma_{\text{leptons}} + \Gamma_{\text{neutrinos}}, \tag{3.41}$$

where the first two terms on the right are the measured decay rates to hadrons and charged leptons, respectively. Although the rate to neutrinos Γ_ν is not directly measured, it can be calculated in the standard model and combining this with experimental data for the other decay modes, a value of N_ν may be found. The best value using all available data is $N_\nu = 3.00 \pm 0.08$, which is consistent with the expectation for three neutrino species, but not four. The conclusion is that only three generations (flavours) of leptons can exist, if we assume universal lepton interactions and exclude very large neutrino masses.

Why there are just three generations of leptons remains a mystery, particularly as the extra two generations seem to tell us nothing fundamental that cannot be deduced from the interaction of the first generation.

3.2 Quarks

We turn now to the strongly interacting particles – the quarks and their bound states, the hadrons. These also interact by the weak and electromagnetic interactions, although such effects can often be neglected compared with the strong interactions. To this extent we are entering the realm of ‘strong interaction physics’.

3.2.1 Evidence for quarks

Several hundred hadrons (not including nuclei) have been observed since pions were first produced in the laboratory in the early 1950s and all have zero or integer electric charges: $0, \pm 1, \text{or} \pm 2$ in units of e. They are all bound states of the fundamental spin-$\frac{1}{2}$ quarks, whose electric charges are either $+\frac{2}{3}$ or $-\frac{1}{3}$, and/or antiquarks, with charges $-\frac{2}{3}$ or $+\frac{1}{3}$. The quarks themselves have never been directly observed as single, free particles and, as remarked earlier, this fact initially made it difficult for quarks to be accepted as anything other than convenient mathematical quantities for performing calculations. Only later, when the fundamental reason for this was realized (it will be discussed in Chapter 6), were quarks universally accepted as physical entities. Nevertheless, there is compelling experimental evidence for their existence. The evidence comes from three main areas: *hadron spectroscopy, lepton scattering* and *jet production.*

Hadron spectroscopy

This is the study of the static properties of hadrons: their masses, lifetimes and decay modes, and especially the values of their quantum numbers, including spin, electric charge and several more that we define in Section 3.2.2. As mentioned in Chapter 1, the existence and properties of quarks were first inferred from hadron spectroscopy by Gell-Mann and independently by Zweig in 1964 and the close correspondence between the experimentally observed hadrons and those predicted by the quark model, which we will examine in more detail later, remains one of the strongest reasons for our belief in the existence of quarks.

Lepton scattering

It was mentioned in earlier chapters that in the early 1960s experiments were first performed where electrons were scattered from protons and neutrons. These strongly suggested that nucleons were not elementary. By the late 1960s this work had been extended to higher energies and with projectiles that included muons and neutrinos. In much the same way as Rutherford deduced the existence of the nucleus in atoms, high-energy lepton scattering, particularly at large momentum transfers, revealed the existence of point-like entities within the nucleons, which we now identify as quarks.

Jet production

High-energy collisions can cause the quarks within hadrons, or newly created quark–antiquark pairs, to fly apart from each other with very high energies. Before they can be observed, these quarks are converted into 'jets' of hadrons (a process referred to as *fragmentation*) whose production rates and angular distributions reflect those of the quarks from which they originated. They were first clearly identified in experiments at the DESY laboratory in Hamburg in 1979, where electrons and positrons were arranged to collide 'head-on' in a magnetic field. An example of a 'two-jet' event is shown in Figure 3.5. The picture is a computer reconstruction of an end view along the beam direction; the solid lines indicate the reconstructed charged particle trajectories taking into account the known magnetic field, which is also parallel to the beam direction; the dotted lines indicate the reconstructed trajectories of neutral particles, which were detected outside this device by other means.

The production rate and angular distribution of the observed jets closely matches that of quarks produced in the reaction

$$e^+ + e^- \to q + \bar{q}, \tag{3.42}$$

by the mechanism of Figure 3.6. Such jets have now been observed in many reactions, and are strong evidence for the existence of quarks within hadrons.

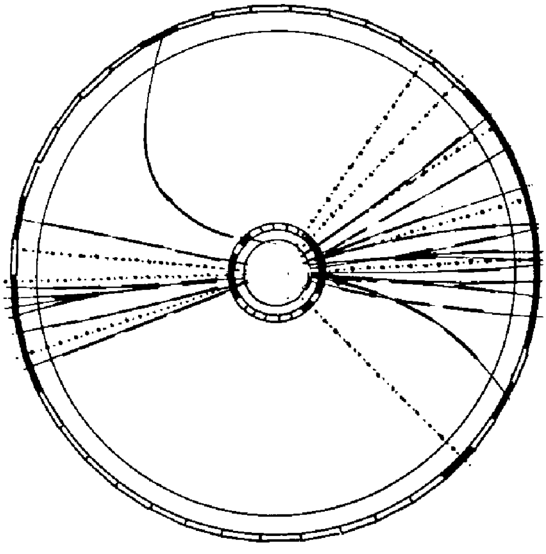

Figure 3.5 Two-jet event in e^+e^- collisions

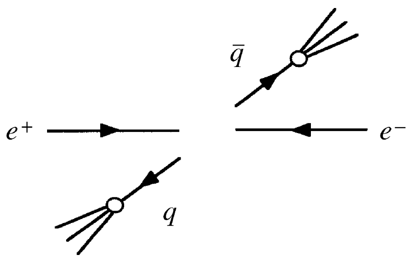

Figure 3.6 Mechanism for two-jet production in e^+e^- annihilation reaction

The failure to detect free quarks is not an experimental problem. Firstly, free quarks would be easily distinguished from other particles by their fractional charges and their resulting ionization properties.[12] Secondly, electric charge conservation implies that a fractionally charged particle cannot decay to a final state composed entirely of particles with integer electric charges. Hence the lightest fractionally charged particle, i.e. the lightest free quark, would be stable and so presumably easy to observe. Finally, some of the quarks are not very massive (see below) and because they interact by the strong interaction, one would expect free quarks to be copiously produced in, for example, high-energy proton–proton collisions. However, despite careful and exhaustive searches in ordinary matter, in cosmic rays and in high-energy collision products, free quarks have

[12]We will see in Chapter 4 that energy losses in matter due to ionization are proportional to the square of the charge and thus would be 'anomalously' small for quarks.

never been observed. The conclusion – that quarks exist solely within hadrons and not as isolated free particles – is called *confinement.* It is for this reason that we are forced to study the properties of hadrons, the bound states of quarks.

The modern theory of strong interactions, called *quantum chromodynamics* (*QCD*), which is discussed in Chapter 5, offers at least a qualitative account of confinement, although much of the detail eludes us due to the difficulty of performing accurate calculations. In what follows, we shall assume confinement and use the properties of quarks to interpret the properties of hadrons.

3.2.2 Quark generations and quark numbers

Six distinct types, or *flavours*, of spin-$\frac{1}{2}$ quarks are now known to exist. Like the leptons, they occur in pairs, or *generations*, denoted

$$\begin{pmatrix} u \\ d \end{pmatrix}, \quad \begin{pmatrix} c \\ s \end{pmatrix}, \quad \begin{pmatrix} t \\ b \end{pmatrix}. \tag{3.43}$$

Each generation consists of a quark with charge $+\frac{2}{3}$ (u, c, or t) together with a quark of charge $-\frac{1}{3}$ (d, s, or b), in units of e. They are called the *down* (d), *up* (u), *strange* (s), *charmed* (c), *bottom* (b) and *top* (t) quarks. The quantum numbers associated with the s, c, b and t quarks are called *strangeness, charm, beauty* and *truth*, respectively. The antiquarks are denoted

$$\begin{pmatrix} \bar{d} \\ \bar{u} \end{pmatrix}, \quad \begin{pmatrix} \bar{s} \\ \bar{c} \end{pmatrix}, \quad \begin{pmatrix} \bar{b} \\ \bar{t} \end{pmatrix} \tag{3.44}$$

with charges $+\frac{1}{3}$ ($\bar{d}$, $\bar{s}$, or $\bar{b}$) and $-\frac{2}{3}$ ($\bar{u}$, $\bar{c}$, $\bar{t}$).

Approximate quark masses are given in Table 3.2. Except for the top quark, these masses are inferred indirectly from the observed masses of their hadron

Table 3.2 Properties of quarks: all have spin $\frac{1}{2}$ and masses are given units of GeV/c^2; the antiparticles (not shown) have the same masses as their associated particles, but the electric charges (Q) are reversed in sign (in the major decay modes, X denotes other particles)

Name	Symbol	Mass	Q	Lifetime (s)	Major decays
Down	d	$m_d \approx 0.3$	$-1/3$		
Up	u	$m_u \approx m_d$	$2/3$		
Strange	s	$m_s \approx 0.5$	$-1/3$	10^{-8}–10^{-10}	$s \to u + X$
Charmed	c	$m_c \approx 1.5$	$2/3$	10^{-12}–10^{-13}	$c \to s + X$
					$c \to d + X$
Bottom	b	$m_b \approx 4.5$	$-1/3$	10^{-12}–10^{-13}	$b \to c + X$
Top	t	$m_t = 180 \pm 12$	$2/3$	$\sim 10^{-25}$	$t \to b + X$

bound states, together with models of quark binding.[13] In this context they are also referred to as *constituent* quark masses.

The stability of quarks in hadrons – like the stability of protons and neutrons in atomic nuclei – is influenced by their interaction energies. However, for the s, c and b quarks these effects are small enough for them to be assigned approximate lifetimes of 10^{-8}–10^{-10} s for the s quark and 10^{-12}–10^{-13} s for both the c and b quarks. The top quark is much heavier than the other quarks and its lifetime is of the order of 10^{-25} s. This lifetime is so short that when top quarks are created they decay too quickly to form observable hadrons. In contrast to the other quarks, our knowledge of the top quark is based entirely on observations of its decay products.

When we talk about 'the decay of quarks' we always mean that the decay takes place within a hadron, with the other bound quarks acting as 'spectators', i.e. not taking part in the interaction. Thus, for example, in this picture neutron decay at the quark level is given by the Feynman diagram of Figure 3.7 and no free quarks are observed. Note that it is assumed that the exchanged particle interacts with only one constituent quark in the nucleons. This is the essence of the *spectator model*. (This is not dissimilar to the idea of a single nucleon decaying within a radioactive nucleus.)

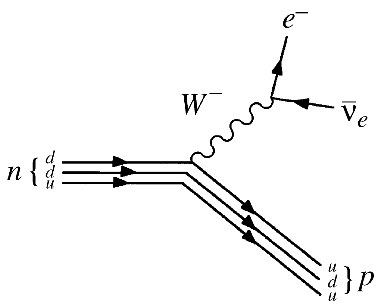

Figure 3.7 Spectator model quark Feynman diagram for the decay $n \to pe^-\bar{\nu}_e$

In strong and electromagnetic interactions, quarks can only be created or destroyed as particle–antiparticle pairs, just like electrons as we discussed in Section 3.1.1. This implies, for example, that in electromagnetic processes corresponding to the Feynman diagram of Figure 3.8, the reaction $e^+ + e^- \to c + \bar{c}$, which creates a $c\bar{c}$ pair, is allowed, but the reaction $e^+ + e^- \to c + \bar{u}$ producing a $c\bar{u}$ pair, is forbidden.[14]

More generally, it implies conservation of each of the six *quark numbers*

$$N_f \equiv N(f) - N(\bar{f}) \qquad (f = u,\ d,\ s,\ c,\ b,\ t) \tag{3.45}$$

where $N(f)$ is the number of quarks of flavour f present and $N(\bar{f})$ is the number of antiquarks of flavour $\bar{f}$ present. For example, for single-particle states; $N_c = 1$ for the

[13] An analogy would be to deduce the mass of nucleons from the masses of nuclei via a model of the nucleus.
[14] Again, these reactions and associated Feynman diagrams do not imply that free quarks are created. Spectator quarks are implicitly present to form hadrons in the final state.

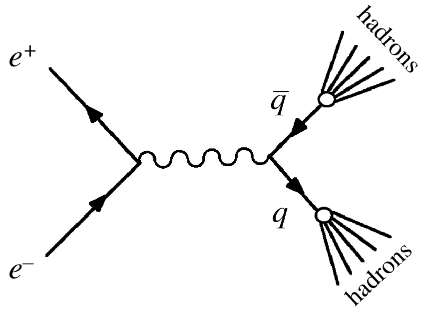

Figure 3.8 Production mechanism for the reaction $e^+e^- \to q\bar{q}$

c quark; $N_c = -1$ for the $\bar{c}$ antiquark; and $N_c = 0$ for all other particles. Similar results apply for the other quark numbers N_f, and for multi-particle states the quark numbers of the individual particles are simply added. Thus a state containing the particles u, u, d, has $N_u = 2$, $N_d = 1$ and $N_f = 0$ for the other quark numbers with $f = s, c, b, t$.

In weak interactions, more general possibilities are allowed, and only the total quark number

$$N_q \equiv N(q) - N(\bar{q}) \tag{3.46}$$

is conserved, where $N(q)$ and $N(\bar{q})$ are the total number of quarks and antiquarks present, irrespective of their flavour. This is illustrated by the decay modes of the quarks themselves, some of which are listed in Table 3.2, which are all weak interaction processes, and we have seen it also in the decay of the neutron in Figure 3.7. Another example is the *main* decay mode of the charmed quark, which is

$$c \to s + u + \bar{d}, \tag{3.47}$$

in which a c quark is replaced by an s quark and a u quark is created together with a $\bar{d}$ antiquark. This clearly violates conservation of the individual quark numbers N_c, N_s, N_u and N_d, but the total quark number N_q is conserved.

In practice, it is convenient to replace the total quark number N_q in analyses by the *baryon number*, defined by

$$B \equiv N_q/3 = [N(q) - N(\bar{q})]/3. \tag{3.48}$$

Like the electric charge and the lepton numbers introduced in the last section, the baryon number is conserved in *all known interactions*, and unlike the lepton number, there are no experiments that suggest otherwise.[15]

[15]However, there are *theories* beyond the standard model that predict baryon number non-conservation, although there is no experimental evidence to support this prediction. These will be discussed briefly in Chapter 9.

3.3 Hadrons

In principle, the properties of atoms and nuclei can be explained in terms of their proton, neutron and electron constituents, although in practice many details are too complicated to be accurately calculated. However, the properties of these constituents can be determined without reference to atoms and nuclei by studying them directly as free particles in the laboratory. In this sense atomic and nuclear physics are no longer fundamental, although they are still very interesting and important if we want to understand the world we live in.

In the case of hadrons, the situation is more complicated. Their properties are explained in terms of a few fundamental quark constituents; but the properties of the quarks themselves can only be studied experimentally by appropriate measurements on hadrons. Whether we like it or not, studying quarks without hadrons is not an option.

3.3.1 Flavour independence and charge multiplets

One of the most fundamental properties of the strong interaction is *flavour independence*. This is the statement that the strong force between two quarks at a fixed distance apart is independent of which quark flavours $u,\ d,\ s,\ c,\ b,\ t$ are involved. Thus, for example, the strong forces between us and ds pairs are identical. The same principle applies to quark–antiquark forces which are, however, *not* identical to quark–quark forces, because in the former case annihilations can occur. Flavour independence does not apply to the electromagnetic interaction, since the quarks have different electric charges, but compared with the strong force between quarks, the electromagnetic force is a small correction. In addition, in applying flavour independence one must take proper account of the quark mass differences, which can be non-trivial. However, there are cases where these corrections are small or easily estimated, and the phenomenon of flavour independence is plain to see.

One consequence of flavour independence is the striking observation that hadrons occur in families of particles with approximately the same masses, called *charge multiplets*. Within a given family, all particles have the same spin-parity and the same baryon number, strangeness, charm and beauty, but differ in their electric charges. Examples are the triplet of pions, $(\pi^+,\ \pi^0,\ \pi^-)$ and the nucleon doublet $(p,\ n)$. The latter behaviour reflects an approximate symmetry between u and d quarks. This arises because, as we shall see in Section 3.3.2, these two quarks have only a very small mass difference

$$m_d - m_u = (3 \pm 1)\mathrm{MeV/c^2}, \tag{3.49}$$

so that in this case mass corrections can to a good approximation be neglected. For example, consider the proton and neutron. We shall see in the next section that their quark content is $p(938) = uud$ and $n(940) = udd$. If we neglect the small mass difference between the u and d quarks and also the electromagnetic interactions, which is equivalent to setting all electric charges to zero, so that the forces acting on the u and d quarks are exactly equal, then replacing the u quark by a d quark in the proton would produce a 'neutron' which would be essentially identical to the proton. Of course the symmetry is not exact because of the small mass difference between the u and d quark*s* and because of the electromagnetic forces, and it is these that give rise to the small differences in mass within multiplets.

Flavour independence of the strong forces between u and d quarks also leads directly to the *charge independence of nuclear forces*, e.g. the equality of the force between any pair of nucleons, provided the two particles are in the same spin state. Subsumed in the idea of charge independence is the idea of *charge symmetry*, i.e. the equality of the proton–proton and neutron–neutron forces, again provided the two particles are in the same spin state. Evidence for the latter is found in studies of nuclei with the same value of A, but the values of N and Z interchanged (*mirror nuclei*). An example is shown in Figure 3.9. The two nuclei ${}^{11}_{5}\mathrm{B}$ and ${}^{11}_{6}\mathrm{C}$ have the same number of np pairs, but ${}^{11}_{5}\mathrm{B}$ has 10 pp pairs and 15 nn pairs, whereas ${}^{11}_{6}\mathrm{C}$ has 15 pp pairs and 10 nn pairs. Thus, allowing for the Coulomb interaction, the approximate equality of the level structures of these two nuclei, as seen in Figure 3.9, means *charge symmetry* is approximately verified. To test charge independence in a nuclear context we would have to look at the level structure in three related nuclei such as ${}^{11}_{4}\mathrm{Be}$, ${}^{11}_{5}\mathrm{B}$ and ${}^{11}_{6}\mathrm{C}$.

Here the test is not so clear-cut because an np pair is not subject to the restrictions of the Pauli principle like pp and nn pairs and there is evidence (to be discussed briefly in Chapter 7) that the np force is stronger in the $S = 1$ state than in the $S = 0$ state. Nevertheless, the measured energy levels in such triplets of nuclei support the idea of approximate charge independence of nuclear forces.

The symmetry between u and d quarks is called *isospin symmetry* and greatly simplifies the interpretation of hadron physics. It is described by the same mathematics as ordinary spin, hence the name. For example, the proton and neutron are viewed as the 'up' and 'down' components of a single particle, the nucleon N, that has an isospin quantum number $\mathbf{I} = \frac{1}{2}$, with I_3 values $\frac{1}{2}$ and $-\frac{1}{2}$, assigned to the proton and neutron, where I_3 is analogous to the magnetic quantum number in the case of ordinary spin. Likewise, the three pions π^+, π^- and π^0 are part of a triplet π with $\mathbf{I} = 1$ corresponding to I_3 values 1, 0 and -1, respectively. In discussing the strong interactions between pions and nucleons, it is then only necessary to consider the πN interaction with total isospin either $\frac{1}{2}$ or $\frac{3}{2}$.

As an example, we will consider some predictions for the hadronic resonance $\Delta(1232)$. The $\Delta(1232)$ has $\mathbf{I} = \frac{3}{2}$ and four charge states Δ^{++}, Δ^{+}, Δ^{0} and Δ^{-} (see Table 3.3) corresponding to $I_3 = \frac{3}{2}, \frac{1}{2}, -\frac{1}{2}, -\frac{3}{2}$, respectively. If we use the notation $|\pi N; I, I_3\rangle$ for a πN state, then $\left|\pi N; \frac{3}{2}, \frac{3}{2}\right\rangle$ is the unique state $\pi^+ p$ and may be written

$$\left|\pi N; \frac{3}{2}, \frac{3}{2}\right\rangle = \left|\pi; 1, 1\right\rangle \left|N; \frac{1}{2}, \frac{1}{2}\right\rangle. \tag{3.50}$$

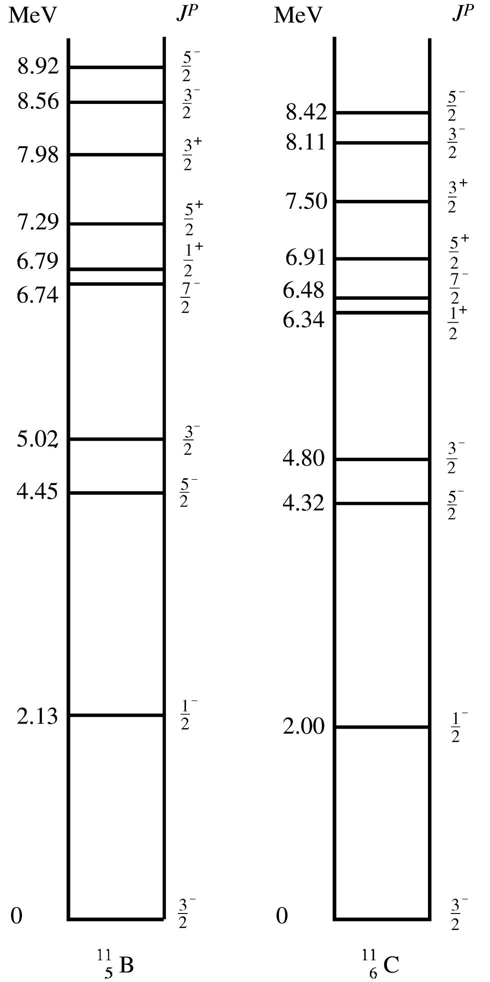

Figure 3.9 Low-lying energy levels with spin-parity J^P of the mirror nuclei ${}^{11}_{5}\mathrm{B}$ and ${}^{11}_{6}\mathrm{C}$. (data from Aj90)

The other πN states may then be obtained by applying quantum mechanical shift (ladder) operators to Equation (3.50), as is done when constructing ordinary spin states. This gives[16]

$$\left|\pi N; \frac{3}{2}, \frac{1}{2}\right\rangle = -\sqrt{\frac{1}{3}}\left|\pi^+ n\right\rangle + \sqrt{\frac{2}{3}}\left|\pi^0 p\right\rangle \tag{3.51}$$

and hence isospin invariance predicts

$$\frac{\Gamma(\Delta^+ \to \pi^+ n)}{\Gamma(\Delta^+ \to \pi^0 p)} = \frac{1}{2}, \tag{3.52}$$

which is in good agreement with experiment.

[16]The reason for the minus sign and other details are given in, for example, Appendix D of Ma97.

Secondly, by constructing all the πN isospin states by analogy with Equations (3.50) and (3.51) we can show that

$$\left|\pi^- p\right\rangle = \frac{1}{\sqrt{3}}\left|\pi N; \frac{3}{2}, -\frac{1}{2}\right\rangle - \sqrt{\frac{2}{3}}\left|\pi N; \frac{1}{2}, -\frac{1}{2}\right\rangle \tag{3.53a}$$

and

$$\left|\pi^0 n\right\rangle = \sqrt{\frac{2}{3}}\left|\pi N; \frac{3}{2}, -\frac{1}{2}\right\rangle + \frac{1}{\sqrt{3}}\left|\pi N; \frac{1}{2}, -\frac{1}{2}\right\rangle. \tag{3.53b}$$

Then, if M_I is the amplitude for scattering in a pure isospin state I,

$$M(\pi^- p \to \pi^- p) = \frac{1}{3}M_3 + \frac{2}{3}M_1 \tag{3.54a}$$

and

$$M(\pi^- p \to \pi^0 n) = \frac{\sqrt{2}}{3}M_3 - \frac{\sqrt{2}}{3}M_1. \tag{3.54b}$$

At the $\Delta(1232)$, the available energy is such that the total cross-section is dominated by the elastic ($\pi^- p \to \pi^- p$) and charge-exchange ($\pi^- p \to \pi^0 n$) reactions. In addition, because the $\Delta(1232)$ has $\mathbf{I} = \frac{3}{2}$, $M_3 \gg M_1$, so

$$\sigma_{\text{total}}(\pi^- p) = \sigma(\pi^- p \to \pi^- p) + \sigma(\pi^- p \to \pi^0 n) \propto \frac{1}{3}|M_3|^2 \tag{3.55a}$$

and

$$\sigma_{\text{total}}(\pi^+ p) \propto |M_3|^2. \tag{3.55b}$$

Thus, neglecting small kinematic corrections due to mass differences (phase space corrections), isospin symmetry predicts

$$\frac{\sigma_{\text{total}}(\pi^+ p)}{\sigma_{\text{total}}(\pi^- p)} = 3. \tag{3.56}$$

Figure 3.10 shows the two total cross-sections at low energies. There are clear peaks with Breit–Wigner forms at a mass of 1232 MeV corresponding to the production of the $\Delta(1232)$ and the ratio of the peaks is in good agreement with the prediction of Equation (3.56).

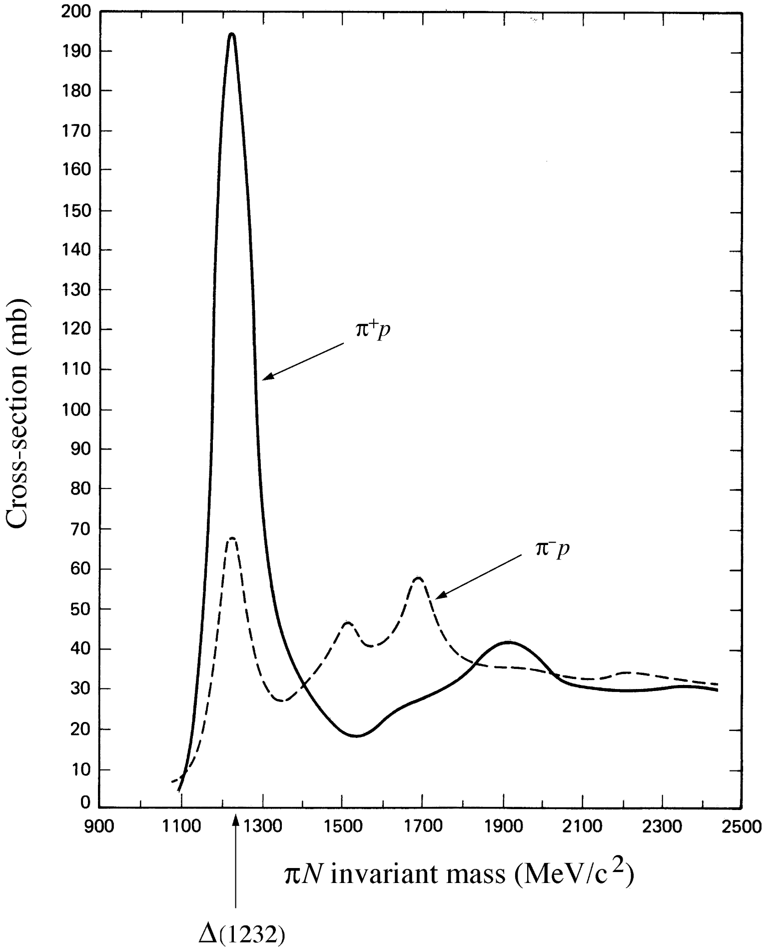

Figure 3.10 Total cross-sections for $\pi^- p$ and $\pi^+ p$ scattering

3.3.2 Quark model spectroscopy

The observed hadrons are of three types. There are *baryons* and their antiparticles *antibaryons*, which have half-integral spin, and *mesons*, which have integral spin. In the *quark model of hadrons* the baryons are assumed to be bound states of three quarks ($3q$), *antibaryons* are assumed to be bound states of three antiquarks ($3\bar{q}$) and *mesons* are assumed to be bound states of a quark and an antiquark ($q\bar{q}$).[17] The

[17]In addition to these so-called 'valence' quarks there could also, in principle, be other constituent quarks present in the form of a cloud of virtual quarks and antiquarks – the so-called 'sea' quarks – the origin of which we will discuss in Chapter 5. In this chapter we consider only the valence quarks which determine the static properties of hadrons. The masses of the constituent quarks could be quite different from those that appear in the fundamental strong interaction Hamiltonian for quark–quark interactions via gluon exchange (i.e. QCD), because those quarks are free of the dynamical effects experienced in hadrons. The latter are referred to as 'current' quarks.

baryons and antibaryons have baryon numbers 1 and -1 respectively, while the mesons have baryon number 0. Hence the baryons and antibaryons can annihilate each other in reactions which conserve baryon number to give mesons or, more rarely, photons or lepton–antilepton pairs, in the final state.

The lightest known baryons are the proton and neutron, with the quark compositions given in Section 3.3.1:

$$p = uud \quad \text{and} \quad n = udd. \tag{3.57}$$

These particles have been familiar as constituents of atomic nuclei since the 1930s. The birth of particle physics as a new subject, distinct from atomic and nuclear physics, dates from 1947, when hadrons other than the neutron and proton were first detected. These were the *pions*, already mentioned, and the *kaons*, discovered in cosmic rays by groups in Bristol and Manchester Universities, UK, respectively.

The discovery of the pions was not totally unexpected, since Yukawa had famously predicted their existence and their approximate masses in 1935, in order to explain the observed range of nuclear forces (recall the discussion in Section 1.5.2). This consisted of finding what mass was needed in the Yukawa potential to give the observed range of the strong nuclear force (which was poorly known at the time). After some false signals, a particle with the right mass and suitable properties was discovered – this was the pion. Here and in what follows we will give the hadron masses in brackets in units of MeV/c^2 and use a superscript to indicate the electric charge in units of e. Thus the pions are $\pi^{\pm}(140)$, $\pi^0(135)$. Pions are the lightest known mesons and have the quark compositions

$$\pi^+ = u\bar{d}, \quad \pi^0 = u\bar{u},\ d\bar{d}, \quad \pi^- = d\bar{u}. \tag{3.58}$$

While the charged pions have a unique composition, the neutral pion is composed of both $u\bar{u}$ and $d\bar{d}$ pairs in equal amounts. Pions are copiously produced in high-energy collisions by strong interaction processes such as $p + p \to p + n + \pi^+$.

In contrast to the discovery of the pions, the discovery of the kaons was totally unexpected, and they were almost immediately recognized as a completely new form of matter, because they had supposedly 'strange' properties. Eventually, after several years, it was realized that these properties were precisely what would be expected if kaons had non-zero values of a hitherto unknown quantum number, given the name *strangeness*, which was conserved in strong and electromagnetic interactions, but not necessarily conserved in weak interaction. Particles with non-zero strangeness were named *strange particles*, and with the advent of the quark model in 1964, it was realized that strangeness S was, apart from a sign, the strangeness quark number introduced earlier, i.e.

$$S = -N_s. \tag{3.59}$$

Kaons are the lightest strange mesons, with the quark compositions:

$$K^+(494) = u\bar{s} \quad \text{and} \quad K^0(498) = d\bar{s}, \tag{3.60}$$

where K^+ and K^0 have $S = +1$ and their antiparticles K^- and $\bar{K}^0$ have $S = -1$, while the lightest strange baryon is the *lambda*, with the quark composition $\Lambda = uds$. Subsequently, hadrons containing c and b quarks have also been discovered, with non-zero values of the *charm* and *beauty* quantum numbers defined by

$$C \equiv N_c \equiv N(c) - N(\bar{c}) \quad \text{and} \quad \tilde{B} \equiv -N_b \equiv -N(b) - N(\bar{b}). \tag{3.61}$$

The above examples illustrate just some of the many different combinations of quarks that form baryons or mesons. These and some further examples are shown in Table 3.3 and a complete listing is given in the PDG Tables.

Table 3.3 Some examples of baryons and mesons, with their major decay modes; masses are in MeV/c^2

Particle	Mass	Lifetime (s)	Major decays
$\pi^+(u\bar{d})$	140	2.6×10^{-8}	$\mu^+\nu_\mu$ ($\sim$100%)
$\pi^0(u\bar{u}, d\bar{d})$	135	8.4×10^{-17}	$\gamma\gamma$ ($\sim$100%)
$K^+(u\bar{s})$	494	1.2×10^{-8}	$\mu^+\nu_\mu$ (64%)
			$\pi^+\pi^0$ (21%)
$K^{*+}(u\bar{s})$	892	$\sim 1.3 \times 10^{-23}$	$K^+\pi^0$, $K^0\pi^+$ ($\sim$100%)
$D^-(d\bar{c})$	1869	1.1×10^{-12}	Several seen
$B^-(b\bar{u})$	5278	1.6×10^{-12}	Several seen
$p(uud)$	938	Stable	None
$n(udd)$	940	887	$pe^-\bar{\nu}_e$ (100%)
$\Lambda(uds)$	1116	2.6×10^{-10}	$p\pi^-$ (64%)
			$n\pi^0$ (36%)
$\Delta^{++}(uuu)$	1232	$\sim 0.6 \times 10^{-23}$	$p\pi^+$ (100%)
$\Omega^-(sss)$	1672	0.8×10^{-10}	ΛK^- (68%)
			$\Xi^0\pi^-$ (24%)
$\Lambda_c^+(udc)$	2285	2.1×10^{-13}	Several seen

To proceed more systematically one could, for example, construct all the mesons states of the form $q\bar{q}$, where q can be any of the six quark flavours. Each of these is labelled by its spin and its intrinsic parity P. The simplest such states would have the spins of the two quarks antiparallel with no orbital angular momentum between them and so have spin-parity $J^P = 0^-$. (Recall from Chapter 1 that quarks and antiquarks have opposite parities.) If, for simplicity, we consider those states composed of just u, d and s quarks, there will be nine such mesons and they have quantum numbers which may be identified with the observed mesons (K^0, K^+), $(\bar{K}^0, K^-)$, $(\pi^\pm, \pi^0)$ and two neutral particles, which are called η and η'. This *supermultiplet* is shown Figure 3.11(a) as a plot of Y, the *hypercharge*, defined as

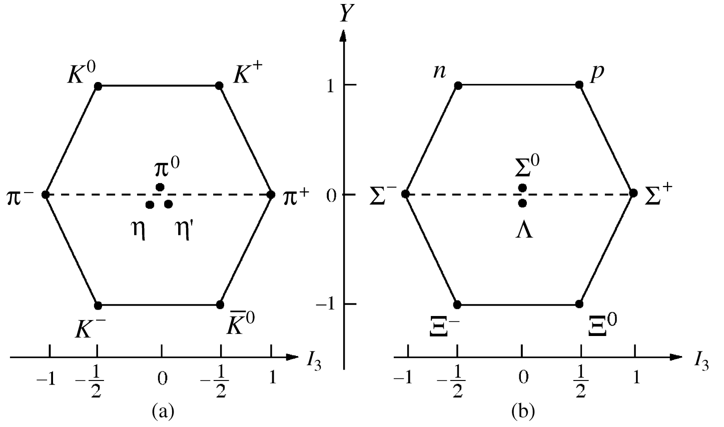

Figure 3.11 The lowest-lying states with (a) $J^P = 0^-$ and (b) $J = \frac{1}{2}^+$ that are composed of u, d and s quarks

$Y \equiv B + S + C + \tilde{B} + T$, against I_3, the third component of isospin. This can be extended to the lowest-lying qqq states and the lowest-lying supermultiplet consists of the eight $J^P = \frac{1}{2}^+$ baryons shown in Figure 3.11(b).[18]

It is a remarkable fact that the states observed experimentally agree with those predicted by the simple combinations qqq, $\bar{q}\bar{q}\bar{q}$ and $q\bar{q}$ and until very recently there was no evidence for states corresponding to any other combinations. However, some recent experiments have claimed evidence for the existence of a few states outside this scheme, possibly ones involving five quarks, although other experiments have failed to confirm this. Nevertheless, it is still a fact that hadron states are overwhelmingly composed of the simplest quark combinations of the basic quark model. This was one of the original pieces of evidence for the existence of quarks and remains one of the strongest today.

The scheme may also be extended to more quark flavours, although the diagrams become increasingly complex. For example, Figure 3.12 shows the predicted $J^P = \frac{3}{2}^+$ baryon states formed from u, d, s and c quarks when all three quarks have their spins aligned, but still with zero orbital angular momentum between them. All the states in the bottom plane have been detected as well as many in the higher planes and with the possible exception of the five-quark states mentioned previously, no states have been found that are outside this scheme. The latest situation may be found in the PDG Tables.

For many quark combinations there exist not one, but several states. For example, the lowest-lying state of the $u\bar{d}$ system has spin-parity 0^- and is the π^+ meson. It can be regarded as the 'ground state' of the $u\bar{d}$ system. Here the spins of the quark

[18]If you try to try to verify Figure 3.11, you will find that it is necessary to assume that the overall hadronic wavefunctions $\Psi = \psi_{\text{space}}\psi_{\text{spin}}$ are *symmetric* under the exchange of identical quarks, i.e. opposite to the symmetry required by the Pauli principle. This apparent contradiction will be resolved in Chapter 5.

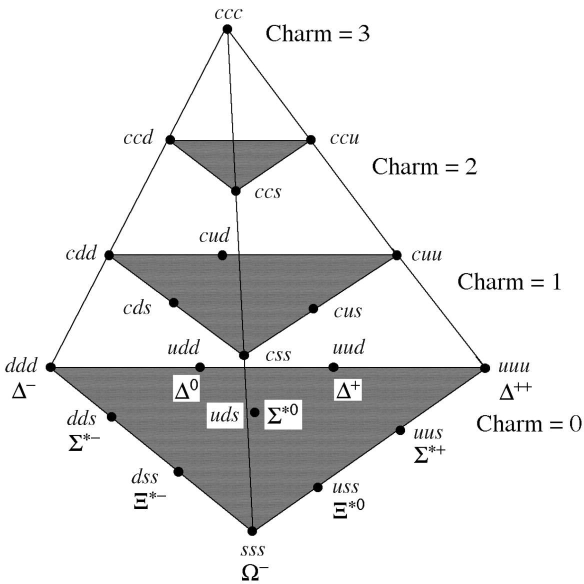

Figure 3.12 The $J = \frac{3}{2}^+$ baryon states composed of u, d, s and c quarks

constituents are anti-aligned to give a total spin $\mathbf{S} = \mathbf{0}$ and there is no orbital angular momentum $\mathbf{L}$ between the two quarks, so that the total angular momentum, which we identify as the spin of the hadron, is $\mathbf{J} = \mathbf{L} + \mathbf{S} = \mathbf{0}$. Other 'excited' states can have different spin-parities depending on the different states of motion of the quarks within the hadron.

An example is the $K^{*+}(890)$ meson shown in Table 3.3 with $J^P = 1^-$. In this state the u and $\bar{s}$ quarks have their spins aligned so that $\mathbf{S} = \mathbf{1}$ and there is no orbital angular momentum between them, i.e. $\mathbf{L} = \mathbf{0}$, so that the spin of the K^{*+} is $\mathbf{J} = \mathbf{L} + \mathbf{S} = \mathbf{1}$. This is a *resonance* and such states usually decay by the strong interaction, with very short lifetimes, of order 10^{-23} s. The mass distribution of their decay products is described by the Breit–Wigner formula we met in Section 1.6.3. The spin of a resonance may be found from an analysis of the angular distributions of its decay products. This is because the distribution will be determined by the wavefunction of the decaying particle and this will contain an angular part proportional to a spherical harmonic labelled by the orbital angular momentum between the decay products. Thus from a measurement of the angular distribution of the decay products, the angular momentum may be found, and hence the spin of the resonance. It is part of the triumph of the quark model that it successfully accounts for the excited states of the various quark systems, as well as their ground states, when the internal motion of the quarks is properly taken into account.

From experiments such as electron scattering we know that hadrons have typical radii r of the order of 1 fm and hence associated time scales r/c of the order of 10^{-23} s. The vast majority are highly unstable resonances, corresponding to excited states of the various quark systems, and decay to lighter hadrons by the strong interaction, with lifetimes of this order. The $K^{*+}(890) = u\bar{s}$ resonance, mentioned above, is an example. It decays to $K^+\pi^0$ and $K^0\pi^+$ final states with a lifetime of 1.3×10^{-23} s. The quark description of the process $K^{*+} \to K^0 + \pi^+$, for example, is

$$u\bar{s} \to d\bar{s} + u\bar{d}. \tag{3.62}$$

From this we see that the final state contains the same quarks as the initial state, plus an additional $d\bar{d}$ pair, so that the quark numbers N_u and N_d are separately conserved. This is characteristic of strong and electromagnetic processes, which are only allowed if each of the quark numbers $N_u,\ N_d,\ N_s,\ N_c$ and N_b is separately conserved.

Since leptons and photons do not have strong interactions, hadrons can only decay by the strong interaction if lighter states composed solely of other hadrons exist with the same quantum numbers. While this is possible for the majority of hadrons, it is not in general possible for the lightest state corresponding to any given quark combination. These hadrons, which cannot decay by strong interactions, are long-lived on a timescale of the order of 10^{-23} s and are often called *stable particles.* It is more accurate to call them *long-lived particles*, because except for the proton they are not absolutely stable, but decay by either the electromagnetic or weak interaction.

The proton is stable because it is the lightest particle with non-zero baryon number and baryon number is conserved in all known interactions. A few of the other long-lived hadrons decay by electromagnetic interactions to final states that include photons. These decays, like the strong interaction, conserve all the individual quark numbers. An example of this is the neutral pion, which has $N_u = N_d = N_s = N_c = N_b = 0$ and decays by the reaction

$$\pi^0(u\bar{u},\ d\bar{d}) \to \gamma + \gamma, \tag{3.63}$$

with a lifetime of 0.8×10^{-16} s. However, most of the long-lived hadrons have non-zero values for at least one of the quark numbers, and can only decay by the weak interaction, in which quark numbers do not have to be conserved. For example, the positive pion decays with a lifetime of 2.6×10^{-8} s by the reaction

$$\pi^+ \to \mu^+ + \nu_\mu, \tag{3.64}$$

while the $\Lambda(1116) = uds$ baryon decays mainly by the reactions

$$\Lambda \to p + \pi^- \quad \text{and} \quad n + \pi^0, \tag{3.65}$$

with a lifetime of 2.6×10^{-10} s. The quark interpretations of these reactions are

$$(u\bar{d}) \to \mu^+ + \nu_\mu, \tag{3.66}$$

in which a u quark annihilates with a $\bar{d}$ antiquark, violating both N_u and N_d conservation; and for lambda decay to charged pions,

$$sud \rightarrow uud + d\bar{u}, \tag{3.67}$$

in which an s quark turns into a u quark and a $u\bar{d}$ pair is created, violating N_d and N_s conservation.

We see from the above that the strong, electromagnetic or weak nature of a given hadron decay can be determined by inspecting quark numbers. The resulting lifetimes can then be summarized as follows. Strong decays lead to lifetimes that are typically of the order of 10^{-23} s. Electromagnetic decay rates are suppressed by powers of the fine structure constant α relative to strong decays, leading to observed lifetimes in the range 10^{-16}–10^{-21} s. Finally, weak decays give longer lifetimes, which depend sensitively on the characteristic energy of the decay.

A useful measure of the decay energy is the Q-value, the kinetic energy released in the decay of the particle at rest, which we metioned before in Section 2.3. In the weak interactions of hadrons, Q-values of the order of $10^2 - 10^3$ MeV are typical, leading to lifetimes in the range 10^{-7}–10^{-13} s, but there are some exceptions, notably neutron decay, $n \rightarrow p + e^- + \bar{\nu}_e$, for which

$$Q = m_n - m_p - m_e - m_{\bar{\nu}_e} = 0.79\,\mathrm{MeV} \tag{3.68}$$

is unusually small, leading to a lifetime of about 10^3 s. Thus hadron decay lifetimes are reasonably well understood and span some 27 orders of magnitude, from about 10^{-24} s to about 10^3 s. The typical ranges corresponding to each interaction are summarized in Table 3.4.

Table 3.4 Typical lifetimes of hadrons decaying by the three interactions

Interaction	Lifetimes (s)
Strong	10^{-22}–10^{-24}
Electromagnetic	10^{-16}–10^{-21}
Weak	10^{-7}–10^{-13}

3.3.3 Hadron masses and magnetic moments

The quark model can make predictions for hadronic magnetic moments and masses in a way that is analogous to the semi-empirical mass formula for nuclear masses, i.e. the formulae have a theoretical basis, but contain parameters that have to be determined from experiment. We start by examining the case of baryon magnetic moments.

These have been measured only for the $\frac{1}{2}^+$ octet of states composed of u, d and s quarks and so we will consider only these. In this supermultiplet, the quarks have zero orbital angular momentum and so the hadron magnetic moments are just the sums of contributions from the constituent quark magnetic moments, which we will assume are of the Dirac form, i.e.

$$\mu_q \equiv \left\langle q, S_z = \frac{1}{2} \middle| \hat{\mu}_z \middle| q, S_z = \frac{1}{2} \right\rangle = e_q e\hbar/2m_q = \left(e_q M_p/m_q\right)\mu_{\mathrm{N}}, \tag{3.69}$$

where e_q is the quark charge in units of e and $\mu_{\mathrm{N}} \equiv e\hbar/2M_p$ is the nuclear magneton. Thus

$$\mu_u = \frac{2M_p}{3m_u}\mu_{\mathrm{N}}, \quad \mu_d = -\frac{M_p}{3m_d}\mu_{\mathrm{N}} \quad \text{and} \quad \mu_s = -\frac{M_p}{3m_s}\mu_{\mathrm{N}}. \tag{3.70}$$

Consider, for example, the case of the $\Lambda(1116) = uds$. It is straightforward to show that the configuration that ensures that the predicted quantum numbers of the supermultiplet agree with experiment is to have the ud pair in a spin-0 state. Hence it makes no contribution to the Λ spin or magnetic moment. Thus we have the immediate prediction

$$\mu_\Lambda = \mu_s = -\frac{M_p}{3m_s}\mu_{\mathrm{N}}. \tag{3.71}$$

For $\frac{1}{2}^+$ baryons B with quark configuration aab, the aa pair is in the symmetric spin-1 state with parallel spins (again this is to ensure that the predicted quantum numbers of the supermultiplet agree with experiment) and magnetic moment $2\mu_a$. The 'spin-up' baryon state is given by

$$\begin{aligned} \left| B; S = \frac{1}{2}, S_z = \frac{1}{2} \right\rangle = & \sqrt{\frac{2}{3}} \left| b; S = \frac{1}{2}, S_z = -\frac{1}{2} \right\rangle \left| aa; S = 1, S_z = 1 \right\rangle \\ & - \sqrt{\frac{1}{3}} \left| b; S = \frac{1}{2}, S_z = \frac{1}{2} \right\rangle \left| aa; S = 1, S_z = 0 \right\rangle \end{aligned} \tag{3.72}$$

The first term corresponds to a state with magnetic moment $2\mu_a - \mu_b$, since the b quark has $S_z = -\frac{1}{2}$; the second term corresponds to a state with magnetic moment μ_b, since the aa pair has $S_z = 0$ and does not contribute. Hence the magnetic moment of B is given by

$$\mu_B = \frac{2}{3}(2\mu_a - \mu_b) + \frac{1}{3}\mu_b = \frac{4}{3}\mu_a - \frac{1}{3}\mu_b. \tag{3.73}$$

For example, the magnetic moment of the proton is

$$\mu_p = \frac{4}{3}\mu_u - \frac{1}{3}\mu_d = \frac{M_p}{m}\mu_{\mathrm{N}}, \tag{3.74}$$

where we have neglected the mass difference between the u and d quarks, as suggested by isospin symmetry, and set $m_u \approx m_d \equiv m$. The predictions for the magnetic moments of all the other members of the $\frac{1}{2}^+$ octet may be found in a similar way in terms of just two parameters, the masses m and m_s. A best fit to the measured magnetic moments (but not taking account of the errors on the data[19]) yields the values $m = 0.344\,\mathrm{GeV/c^2}$ and $m_s = 0.539\,\mathrm{GeV/c^2}$. The predicted moments are shown in Table 3.5. The agreement is good, but by no means perfect and suggests that the assumption that baryons are pure three-quark states with zero orbital angular momentum between them is not exact. For example, there could be small admixtures of states with non-zero orbital angular momentum.

Table 3.5 Magnetic moments of the $\frac{1}{2}^+$ baryon octet as predicted by the constituent quark model, compared with experiment in units of μ_{N}, the nuclear magneton; these have been obtained using $m = 0.344$ GeV/c^2 and $m_s = 0.539$ GeV/c^2 -- errors on the nucleon moments are of the order of 10^{-7}

Particle	Moment	Prediction	Experiment
$p(938)$	$\frac{4}{3}\mu_u - \frac{1}{3}\mu_d$	2.73	2.793
$n(940)$	$\frac{4}{3}\mu_d - \frac{1}{3}\mu_u$	−1.82	−1.913
$\Lambda(1116)$	μ_s	−0.58	-0.613 ± 0.004
$\Sigma^+(1189)$	$\frac{4}{3}\mu_u - \frac{1}{3}\mu_s$	2.62	2.458 ± 0.010
$\Sigma^-(1197)$	$\frac{4}{3}\mu_d - \frac{1}{3}\mu_s$	−1.02	-1.160 ± 0.025
$\Xi^0(1315)$	$\frac{4}{3}\mu_s - \frac{1}{3}\mu_u$	−1.38	-1.250 ± 0.014
$\Xi^-(1321)$	$\frac{4}{3}\mu_s - \frac{1}{3}\mu_d$	−0.47	-0.651 ± 0.003

We now turn to the prediction of hadron masses. The mass differences between members of a given supermulitplet are conveniently separated into the small mass differences between members of the same isospin multiplet and the much larger mass differences between members of different isospin multiplets. The size of the former suggests that they have their origin in electromagnetic effects, and if we neglect them then a first approximation would be to assume that the mass differences are due solely to differences in the constituent quark masses. If we concentrate on hadrons with quark structures composed of u, d and s quarks, since

[19] If we had fitted taking account of the errors, the fit would be dominated by the proton and neutron moments because they have very small errors.

their masses are the best known from experiment, this assumption leads directly to the relations

$$M_{\Xi} - M_{\Sigma} = M_{\Xi} - M_{\Lambda} = M_{\Lambda} - M_N = m_s - m_{u,d} \tag{3.75}$$

for the $\frac{1}{2}^+$ baryon octet and

$$M_{\Omega} - M_{\Xi^*} = M_{\Xi^*} - M_{\Sigma^*} = M_{\Sigma^*} - M_{\Delta} = m_s - m_{u,d} \tag{3.76}$$

for the $\frac{3}{2}^+$ decuplet. These give numerical estimates for $m_s - m_{u,d}$ in the range 120 to 200 $\mathrm{MeV/c^2}$, which are consistent with the estimate from magnetic moments above.

These results support the suggestion that baryon mass differences (and by analogy meson mass differences) are dominantly due to the mass differences of their constituent quarks. However, this cannot be the complete explanation, because if it were then the $\frac{1}{2}^+$ nucleon would have the same mass as the $\frac{3}{2}^+$ $\Delta(1232)$, as they have the same quark constituents, and similarly for other related particles in the $\frac{1}{2}^+$ octet and $\frac{3}{2}^+$ decuplet. The absence of orbital angular momentum in these states means that there is nothing equivalent to the 'fine structure' of atomic physics. The difference lies in the spin structures of these states.

If we take the case of two spin-$\frac{1}{2}$ particles with magnetic moments $\boldsymbol{\mu}_i$ and $\boldsymbol{\mu}_j$ separated by a distance r_{ij} then the interaction energy is proportional to $\boldsymbol{\mu}_i \cdot \boldsymbol{\mu}_j / r_{ij}{}^3$. If, in addition, the particles are point-like and have charges e_i and e_j, the moments will be of the Dirac form $\boldsymbol{\mu}_i = (e_i/m_i)\mathbf{S}_i$. Then for two particles in a relative S-state it can be shown that the interaction energy is given by

$$\Delta E = \frac{8\pi}{3}\frac{e_i e_j}{m_i m_j}|\psi(0)|^2 \mathbf{S}_i \cdot \mathbf{S}_j, \tag{3.77}$$

where $\psi(0)$ is the wavefunction at the origin, $r_{ij} = 0$. (When averaged over all space, the interaction is zero except at the origin.) In atomic physics this is known as the *hyperfine interaction* and causes very small splittings in atomic energy levels. In the hadron case, the electric charges must be replaced by their strong interaction equivalents with appropriate changes to the overall numerical factor. The resulting interaction is called (for reasons that will be clear in Chapter 5) the *chromomagnetic interaction*. As we cannot calculate the equivalent quark–quark wavefunction, for the purposes of a phenomenological analysis we will write the contribution to the hadron mass as

$$\Delta M \propto \frac{\mathbf{S}_1 \cdot \mathbf{S}_2}{m_1 m_2}. \tag{3.78}$$

This of course assumes that $|\psi(0)|^2$ is the same for all states, which will not be exactly true.

Consider first the case of mesons. By writing the total spin squared as

$$\mathbf{S}^2 \equiv (\mathbf{S}_1 + \mathbf{S}_2)^2 = \mathbf{S}_1^2 + \mathbf{S}_2^2 + 2\mathbf{S}_1 \cdot \mathbf{S}_2, \tag{3.79}$$

we easily find the expect values of $\mathbf{S}_1 \cdot \mathbf{S}_2$ are $-\frac{3}{4}\hbar^2$ for the $\mathbf{S} = \mathbf{0}$ (pseudoscalar) mesons and $\frac{1}{4}\hbar^2$ for the $\mathbf{S} = \mathbf{1}$ (vector) mesons. Then the masses may be written

$$M(\text{meson}) = m_1 + m_2 + \Delta M, \tag{3.80}$$

where $m_{1,2}$ are the masses of the constituent quarks and

$$\Delta M(J^P = 0^- \text{ meson}) = -\frac{3a}{4}\frac{1}{m_1 m_2}, \quad \Delta M(J^P = 1^- \text{ meson}) = \frac{a}{4}\frac{1}{m_1 m_2} \tag{3.81}$$

and a is a constant to be found from experiment. The masses of the members of the 0^- and 1^- meson supermultiplets then follow from a knowledge of their quark compositions. For example, the K-mesons have one u or d quark and one s quark and so

$$M_K = m + m_s - \frac{3a}{8}\left(\frac{1}{m^2} + \frac{1}{m_s^2}\right). \tag{3.82}$$

Predictions for the masses of all the mesons are shown in Table 3.6, which also gives the best fit to the measured masses (again ignoring the relative errors on the latter) using these formulae. The predictions correspond to the values

$$m = 0.308\,\text{GeV/c}^2, \quad m_s = 0.482\text{GeV/c}^2, \quad a = 0.0588\ (\text{GeV/c}^2)^3. \tag{3.83}$$

Note that the quark mass values are smaller than those obtained from fitting the baryon magnetic moments. There is no contradiction in this, because there is no reason that quarks should have the same effective masses in mesons as in baryons.

Table 3.6 Meson masses (in Gev/c^2) in the constituent quark model compared with experimental values

Particle	Mass	Prediction	Experiment
π	$2m - \frac{3a}{4m^2}$	0.15	0.137
K	$m + m_s - \frac{3a}{8}\left(\frac{1}{m^2} + \frac{1}{m_s^2}\right)$	0.46	0.496
η	$\frac{2}{3}m + \frac{4}{3}m_s - \frac{a}{4}\left(\frac{1}{m^2} + \frac{2}{m_s^2}\right)$	0.57	0.549
ρ	$2m + \frac{a}{4m^2}$	0.77	0.770
ω	$2m + \frac{a}{4m^2}$	0.77	0.782
K^*	$m + m_s + \frac{a}{8}\left(\frac{1}{m^2} + \frac{1}{m_s^2}\right)$	0.87	0.892
ϕ	$2m_s + \frac{a}{4m_s^2}$	1.03	1.020

The comparison with the measured values is very reasonable, but omitted from the fit is the η' state where the fit is very poor indeed. Unlike the atomic case, the spin–spin interaction in the strong interaction case leads to substantial corrections to the meson masses.

The baryons are somewhat more complicated, because in this case we have three pairs of spin–spin couplings to consider. In general the spin–spin contribution to the mass is

$$\Delta M \propto \sum_{i<j} \frac{\mathbf{S}_i \cdot \mathbf{S}_j}{m_i m_j}, \quad i,j = 1, 3. \tag{3.84}$$

In the case of the $\frac{3}{2}^+$ decuplet, all three quarks have their spins aligned and every pair therefore combines to make spin-1. Thus for example,

$$(\mathbf{S}_1 + \mathbf{S}_2)^2 = \mathbf{S}_1^2 + \mathbf{S}_2^2 + 2\mathbf{S}_1 \cdot \mathbf{S}_2 = 2\hbar^2, \tag{3.85}$$

giving $\mathbf{S}_1 \cdot \mathbf{S}_2 = \hbar^2/4$ and in general

$$\mathbf{S}_1 \cdot \mathbf{S}_2 = \mathbf{S}_1 \cdot \mathbf{S}_3 = \mathbf{S}_2 \cdot \mathbf{S}_3 = \hbar^2/4. \tag{3.86}$$

Using this result, the mass of the $\Sigma^*(1385)$, for example, may be written

$$M_{\Sigma^*} = 2m + m_s + \frac{b}{4}\left(\frac{1}{m^2} + \frac{2}{mm_s}\right), \tag{3.87}$$

where b is a constant to be determined from experiment. (There is no reason for b to be equal to the constant a used in the meson case because the quark wavefunctions and numerical factors in the baryonic equivalent of Equation (3.77) will be different in the two cases.)

In the case of the $\frac{1}{2}^+$ octet, we have

$$(\mathbf{S}_1^2 + \mathbf{S}_2^2 + \mathbf{S}_3^2) = \mathbf{S}_1^2 + \mathbf{S}_2^2 + \mathbf{S}_3^2 + 2(\mathbf{S}_1 \cdot \mathbf{S}_2 + \mathbf{S}_1 \cdot \mathbf{S}_3 + \mathbf{S}_2 \cdot \mathbf{S}_3) = 3\hbar^2/4 \tag{3.88}$$

and hence

$$\mathbf{S}_1 \cdot \mathbf{S}_2 + \mathbf{S}_1 \cdot \mathbf{S}_3 + \mathbf{S}_2 \cdot \mathbf{S}_3 = -3\hbar^2/4. \tag{3.89}$$

In addition, we have to consider the symmetry of the spin wavefunctions of individual hadrons. For example, without proof (this will be given in Chapter 5), the spins of the u and d pair in the Λ must combine to give $\mathbf{S} = \mathbf{0}$. Thus, $(\mathbf{S}_u + \mathbf{S}_d)^2 = 0$, so that $\mathbf{S}_u \cdot \mathbf{S}_d = -3\hbar^2/4$. Then,

$$M_\Lambda = m_u + m_d + m_s + b\left[\frac{\mathbf{S}_u \cdot \mathbf{S}_d}{m_u m_d} + \frac{\mathbf{S}_u \cdot \mathbf{S}_s}{m_u m_s} + \frac{\mathbf{S}_d \cdot \mathbf{S}_s}{m_d m_s}\right]. \tag{3.90}$$

Table 3.7 Baryon masses (in Gev/c^2) in the constituent quark model compared with experimental values

Particle	Mass	Prediction	Experiment
N	$3m - \dfrac{3b}{4m^2}$	0.89	0.939
Λ	$2m + m_s - \dfrac{3b}{4}\left(\dfrac{1}{m^2}\right)$	1.08	1.116
Σ	$2m + m_s + \dfrac{b}{4}\left(\dfrac{1}{m^2} - \dfrac{4}{mm_s}\right)$	1.15	1.193
Ξ	$m + 2m_s + \dfrac{b}{4}\left(\dfrac{1}{m_s^2} - \dfrac{4}{mm_s}\right)$	1.32	1.318
Δ	$3m + \dfrac{3b}{4m^2}$	1.07	1.232
Σ^*	$2m + m_s + \dfrac{b}{4}\left(\dfrac{1}{m} + \dfrac{2}{mm_s}\right)$	1.34	1.385
Ξ^*	$m + 2m_s + \dfrac{b}{4}\left(\dfrac{2}{mm_s} + \dfrac{1}{m_s^2}\right)$	1.50	1.533
Ω	$3m_s + \dfrac{3b}{m_s^2}$	1.68	1.673

Finally, setting $m_u = m_d = m$ and absorbing factors of $\hbar^2$ into the constant b, gives

$$M_\Lambda = 2m + m_s + b\left[\frac{\mathbf{S}_u \cdot \mathbf{S}_d}{m^2} + \frac{(\mathbf{S}_1 \cdot \mathbf{S}_2 + \mathbf{S}_1 \cdot \mathbf{S}_3 + \mathbf{S}_2 \cdot \mathbf{S}_3 - \mathbf{S}_u \cdot \mathbf{S}_d)}{mm_s}\right] = 2m + m_s - \frac{3b}{4m^2}, \tag{3.91}$$

where we have used Equation (3.89). The resulting formulae for all the $\frac{1}{2}^+$ octet and $\frac{3}{2}^+$ decuplet masses are shown in Table 3.7. Also shown are the predicted masses, where for consistency we have used the same quark mass values obtained earlier in fitting baryon magnetic moments, i.e. $m = 0.308\,\mathrm{GeV/c^2}$ and $m_s = 0.482\,\mathrm{GeV/c^2}$, and varied only the parameter b, giving a value $0.0225\ (\mathrm{GeV/c^2})^3$. The fit is quite reasonable and although better fits can be obtained by allowing the masses to vary there is little justification for this, given the approximations of the analysis.

Overall, what we learn from the above is that the constituent quark model is capable of giving a reasonably consistent account of hadron masses and magnetic moments, at least for the low-lying states (the η' is an exception), provided a few parameters are allowed to be found from experiment.

Problems

3.1 Which of the following reactions are allowed and which are forbidden by the conservation laws appropriate to weak interactions?

(a) $\nu_\mu + p \to \mu^+ + n$;

(b) $\nu_e + p \to n + e^- + \pi^+$;

(c) $\Lambda \to \pi^+ + e^- + \bar{\nu}_e$;

(d) $K^+ \to \pi^0 + \mu^+ + \nu_\mu$.

3.2 Draw the lowest-order Feynman diagram at the quark level for the following decays:

(a) $D^- \to K^0 + \pi^-$;

(b) $\Lambda \to p + e^- + \bar{\nu}_e$.

3.3 Consider the following combinations of quantum numbers $(Q,\ B,\ S,\ C,\ \tilde{B})$ where $Q =$ electric charge, $B =$ baryon number, $S =$ strangeness, $C =$ charm and $\tilde{B} =$ beauty:

(a) $(-1, 1, -2, 0, -1)$;

(b) (0, 0, 1, 0, 1).

Which of these possible states are compatible with the postulates of the quark model?

3.4 Consider a scenario where overall hadronic wavefunctions Ψ consist of just spin and space parts, i.e. $\Psi = \psi_{\text{space}}\,\psi_{\text{spin}}$. What would be the resulting multiplet structure of the lowest-lying baryon states composed of $u,\ d$ and s quarks?

3.5 Draw Feynman diagrams at the quark level for the reactions:

(a) $e^+ + e^- \to \bar{B}^0 + B^0$, where B is a meson containing a b-quark;

(b) $\pi^- + p \to K^0 + \Lambda^0$.

3.6 Find the parity P and charge conjugation C values for the ground-state $(J = 0)$ meson π and its first excited $(J = 1)$ state ρ. Why does the charged pion have a longer lifetime than the ρ? Explain also why the decay $\rho^0 \to \pi^+\pi^-$ has been observed, but not the decay $\rho^0 \to \pi^0\pi^0$.

3.7 The particle Y^- can be produced in the strong interaction process $K^- + p \to K^+ + Y^-$. Deduce its baryon number, strangeness, charm and beauty, and using these, its quark content. The $Y^-(1311)$ decays by the reaction $Y^- \to \Lambda + \pi^-$. Give a rough estimate of its lifetime.

3.8 Verify the expression in Table 3.7 for the mass of the $\frac{1}{2}^+\ \Sigma$ baryon, given that the spins of the two non-strange quarks combine to give $\mathbf{S} = \mathbf{1}$.

3.9 Consider the reaction $K^- + p \to \Omega^- + K^+ + K^0$ followed by the sequence of decays

$$\begin{array}{l}\Omega^- \to \Xi^0 + \pi^- \\ \qquad\ \hookrightarrow \pi^0 + \Lambda, \\ \qquad\qquad \hookrightarrow \gamma + \gamma\end{array} \qquad \begin{array}{l}K^+ \to \pi^+ + \pi^0 \\ \qquad\quad \hookrightarrow \mu^+ + \nu_\mu\end{array} \qquad \text{and} \quad K^0 \to \pi^+ + \pi^- + \pi^0$$

Classify each process as strong, weak or electromagnetic and give your reasons.

3.10 Draw the lowest-order Feynman diagram for the decay $K^+ \to \mu^+ + \nu_\mu + \gamma$ and hence deduce the form of the overall effective coupling.

3.11 A KamLAND-type experiment detects $\bar{\nu}_e$ neutrinos at a distance of 200 m from a nuclear reactor and finds that the flux is (90 ± 10) per cent of that expected if there were no oscillations. Assuming maximal mixing and a mean neutrino energy of 3 MeV, use this result to estimate upper and lower bounds on the squared mass of the $\bar{\nu}_e$.

3.12 Comment on the feasibility of the following reactions:

(a) $p + \bar{p} \to \pi^+ + \pi^-$;

(b) $p \to e^+ + \gamma$;

(c) $\Sigma^0 \to \Lambda + \gamma$;

(d) $p + p \to \Sigma^+ + n + K^0 + \pi^+$;

(e) $\Xi^- \to \Lambda + \pi^-$;

(f) $\Delta^+ \to p + \pi^0$.

3.13 Use the results of Section 3.3.1 to deduce a relation between the total cross-sections for the reactions $\pi^- p \to K^0\Sigma^0, \pi^- p \to K^+\Sigma^-$ and $\pi^+ p \to K^+\Sigma^+$ at a fixed energy.

3.14 At a certain energy $\sigma(\pi^+ n) \approx \sigma(\pi^- p)$, whereas $\sigma(K^+ n) \neq \sigma(K^- p)$. Explain this.